Contents

Quantum Chromodynamics

Alfred H. Mueller

Columbia University, New York, NY 10027

Berndt Müller

Duke University, Durham, NC 22708

Claudio Rebbi

Boston University, Boston, MA 02215

Wesley H. Smith

University of Wisconsin, Madison, WI 53705

Working Group Members

M.G. Albrow	*Fermilab*
G.C. Blazey	*Fermilab*
A. Brandt	*Fermilab*
G. Bunce	*Brookhaven National Laboratory*
A.C. Caldwell	*Columbia University*
N.M. Cason	*University of Notre Dame*
N. Christ	*Columbia University*
J. Collins	*Pennsylvania State*
J.M. Conrad	*Columbia University*
L. Dixon	*Stanford Linear Accelerator Center*
S. Ellis	*University of Washington*
G.E. Forden	*University of Arizona*
S.H. Geer	*Fermilab*
W. Guryn	*Brookhaven National Laboratory*
R.T. Hamilton	*Harvard University*
E. Hughes	*Stanford Linear Accelerator Center*
Z. Jin	*Fermilab*
R. Kauffman	*Brookhaven National Laboratory*
G. Kilcup	*Ohio State University*
A.S. Kronfeld	*Fermilab*
G. Levin	*Fermilab*
M.-P. Lombardo	*Univ. of Illinois Urbana-Champaign*
J.P. Mansour	*Michigan State University*
R.L. McCarthy	*SUNY at Stony Brook*
S.A. Mendoza	*SUNY at Stony Brook*
E.J. Mirkes	*University of Wisconsin*
A.H. Mueller	*Columbia University*
D. Muller	*Stanford Linear Accelerator Center*
F.I. Olness	*Southern Methodist University*
J.-W. Qiu	*Iowa State University*
A.A. Bhatti	*Rockefeller University*
F.O. Borcherding	*Fermilab*
R. Brower	*Boston University*
P. Burrows	*Massachusetts Institute of Technology*
J.B. Carroll	*University of California-Los Angeles*
N.-P. Chang	*City College of CUNY*
E. Church	*University of Washington*
J.M. Conrad	*Columbia University*
S.R. Dasu	*University of Wisconsin*
A. Dzierba	*Indiana University*
B.F. Flaugher	*Fermilab*
J.W. Gary	*University of California-Riverside*
W.T. Giele	*Fermilab*
T.J. Hallman	*University of California-Los Angeles*
B. Harris	*SUNY Stony Brook*
J.W. Huston	*Michigan State University*
J.I. Kapusta	*University of Minnesota*
S. Keller	*Florida State University*
E. Kovacs	*Fermilab*
J.F. Lagae	*University of Kentucky*
S.J. Lindenbaum	*Brookhaven National Laboratory*
J.E. Mandula	*U.S. Department of Energy*
R. Mawhinney	*Columbia University*
H. Melanson	*Fermilab*
R. Milner	*Massachusetts Institute of Technology*
J.M. Moss	*Los Alamos National Laboratory*
B. Muller	*Duke University*
J. Negele	*Massachusetts Institute of Technology*
V. Papavassilio	*Argonne National Laboratory*
K. Rajagopal	*Harvard University*

C. Rebbi *Boston University*
W. Smith *University of Wisconsin*
G. Sterman *SUNY at Stony Brook*
D. Toussaint *University of Arizona*
W.-K. Tung *Michigan State University*
A.R. White *Argonne National Laboratory*
B. Wyslouch *Massachusetts Institute of Technology*
S. Sanghera *Cornell University*
H.M. Spinka *Argonne National Laboratory*
P. Stevenson *Rice University*
L. Trueman *Brookhaven National Laboratory*
H. Weerts *Michigan State University*
J. Womersley *Fermilab DØ*
Z. Zhang *SUNY at Stony Brook*

1 Preface

This report of the American Physical Society Division of Particles and Fields Long Range Planning Working Group on Quantum Chromodynamics (QCD) is in large part the result of contributions made in preparation for and during a two day workshop held in Madison, WI on April 9 & 10, 1994. A number of experts in various areas of QCD experiment and theory contributed reports on specific areas and presented talks that covered the present activities in the area, the expected activities that are planned to take place in the next year or so, and the options for future activities in the more long range time scale. These presentations were accompanied with discussions on the important issues for the future of QCD physics. The agenda for the the workshop is given in Appendix A.

2 Introduction and Executive Summary

2.1 The Beginnings

With the discovery of asymptotic freedom in 1973 the development of Quantum Chromodynamics (QCD) as a quantitative theory of the strong interactions began in earnest. The approximate scaling behavior which had been found in deep inelastic electron scattering experiments at SLAC found a natural explanation. The parton model, developed in response to the experimental discovery of scaling, followed naturally from QCD with quarks and gluons being the previously mysterious partons.

However, quarks and gluons were not produced as free particles. The growth of the QCD coupling at long distances suggested that free quarks would have infinite energy and so could only appear in color singlet combinations with other quarks and gluons. That is, quarks are confined. It was quickly realized that quark confinement could only emerge from essentially nonperturbative aspects of QCD. In 1974 lattice QCD was born with the suggestion that one could perform nonperturbative calculations in QCD by taking the continuum limit of a discretized, but gauge invariant,theory on a finite lattice. This lattice gauge theory contained quark confinement in a way which was manifest, so long as the lattice spacing was not too small. That confinement remains as the lattice spacing goes to zero was later verified numerically.

Although quarks and gluons were not supposed to be present as physical particles in QCD they could manifest themselves in a rather direct way as jets of hadrons having nearly the same energy and direction as the parent quarks and gluons. Evidence for quark jets appeared in e^+e^- annihilation experiments at SPEAR while jets, including the gluon, become clearly visible at PETRA. The successful description of three-jet events in e^+e^- annihilation and of scaling violations in inelastic lepton scattering using perturbative calculations established QCD as a successful quantitative theory of the strong interactions.

2.2 The Major Achievements

From the late 1970's to the present there has been an intense activity, both theoretical and experimental, toward developing QCD into a mature and all encompassing theory of the strong interactions. QCD factorization has been established at a semirigorous level and tested, for example, in the comparison of inelastic lepton scattering, μ-pair production and W and Z production. Determinations of the single coupling parameter in QCD, α_S, have been made from experiments using a large variety of independent methods, and a nontrivial consistency has emerged with $\alpha_S(\mathrm{M}_Z)$ now known to about 5 percent. Fixed target deep inelastic muon and neutrino scattering experiments at Fermilab and CERN have measured consistent distributions for the nucleon valence quark, sea quark and gluon constituents and verified their interactions within the QCD framework. The results from ep scattering at HERA are now extending these measurements to much higher Q^2 and lower x, providing new understanding of the gluons. Another new Q^2 and x region is also explored by the Tevatron collider photon measurements.

The accurate measurements of jet cross sections for single jet transverse energies as large as 400 GeV in proton-antiproton collisions at Fermilab has tested QCD predictions to very short distances and ruled out quark substructure down to distances of 1.4×10^{-17}cm. Data on jets at LEP have allowed accurate determinations of α_S, have stimulated important progress in resumming perturbation theory, and have checked predictions of color coherence phenomena in QCD. Striking progress in calculating hadron masses and weak matrix elements as well as much information and understanding about the finite temperature QCD phase transition have been obtained from numerical studies of lattice gauge theory.

2.3 The Future

QCD is a successful theory of the strong interactions which has been tested by confronting theory and experiment in many different ways in both perturbative and nonperturbative regimes. QCD is unique within the standard model of particle physics in that it is a theory which must exist and be internally consistent over all possible energy scales, both in perturbative and nonperturbative domains, at zero temperature and at high temperature. Thus QCD is a theory which deserves a most intense scrutiny in a diverse set of circumstances, and such a scrutiny will certainly be rewarded by exciting surprises and a deeper and more satisfying understanding of this profound theory of matter. Indeed, it is important to make precise tests of QCD in order to check the very framework within which particle physics is viewed. QCD is the only theory where relativistic quantum field theory, as a basis for particle physics, can be tested in a way which goes beyond a few orders of perturbation theory.

While there is much evidence that QCD is the correct theory of the strong interactions there is still a very incomplete understanding of quark confinement, of the high temperature and high density phases of QCD, of the absence or unnatural smallness of strong CP violation, and of how a perturbative (partonic) picture of QCD is connected with nonperturbative regimes, including bound states.

In the next ten years much new progress can be expected in lattice gauge theory calculations as more computing power becomes available and further progress is made in the development of algorithms. The dream of a precise, convincing and reliable calculation of the hadron mass spectrum and of low energy weak matrix elements is perhaps not too far away. The latter will provide important information for the interpretation of data gathered at the B Factories at the end of this decade. Lattice techniques for evaluating α_S, which are already competitive with perturbative derivations, will probably provide the most precise calculation of the strong coupling constant. The derivation of ever more accurate results on high temperature QCD and on the properties of the quark-gluon plasma will complement experimental information to be obtained at heavy ion colliders. New methods of doing nonperturbative QCD calculations, such as discrete light-cone quantization, are providing complementary insights to the field.

New and increasingly more precise jet data are being gathered in e^+e^-, hadron, and ep collisions. Hadron collider data, photoproduction data, and deep inelastic scattering data continue to provide a wealth of precise information on gluon and other parton densities. Comparisons of observations depending on the same underlying mechanisms, such as gluon distributions or colorless exchanges, provided by different measurements, present valuable opportunities to enhance our understanding of QCD. The high precision emerging in these measurements warrants higher order calculations well beyond those that presently exist. Experimentalists should be encouraged to continue to find ingenious techniques and new areas in which consequences of QCD may be explored. Theorists must refine present calculational techniques and develop new and deeper ways of doing perturbation theory to make use of the new experimental information which is becoming available.

Heavy ion reactions at colliders offer the possibility of studying a new phase of QCD at high temperatures and densities such as existed in the early universe. A major challenge here is to understand the transition at early times in the collision from hadronic degrees of freedom through a pre-thermalized system of quarks and gluons to an equilibrated quark-gluon plasma. This is a field where nuclear physics and particle physics merge, and where perturbative physics, nonperturbative physics and phenomenology are essential in order to extract the desired information on high density and high temperature QCD.

Small-x physics involves high-energy scattering in a regime of weak coupling, but where very high parton densities may be achieved leading to a new nonperturbative domain of QCD. Important information has recently been produced by experiments at HERA and relevant data should come soon from the Fermilab Tevatron collider. The rapid increase in parton density with decreasing x observed in ep scattering must eventually be constrained by unitarity. Therefore, future running at HERA should observe effects from the saturation of the parton densities. Low-x physics results would also emerge from LHC. Theoretical progress in this field may come from techniques in mathematical physics and two-dimensional field theories as well as from traditional perturbative and soft physics approaches.

As the US nuclear physics community is moving to explore higher energies at facilities such as CEBAF and RHIC, its interaction with the particle physics community in the field of QCD will intensify. In the future, CEBAF will play an increasingly important role in the study of hadron spectroscopy. Interactions between the nuclear and particle physics communities, *e.g.*, through the shared use of experimental facilities, as already occur at a less extensive scale at Brookhaven, Fermilab, and SLAC, are beneficial to both communities and should be encouraged to expand. In particular, the fixed target program at Fermilab has been very successful and offers an important area for collaboration between nuclear and particle physicists in the future.

While the past decade has been one of much progress in QCD and the same can be expected for the decade to follow, it should be noted that in comparison to the European effort at HERA and LEP the present experimental program in the US suffers from a shortage of experimenters and theorists dedicated to QCD studies as well as organized collaboration between them. The Fermilab Tevatron collider is and will remain a leading facility for QCD studies, and the CDF and DØ collaborations have produced many important QCD results. Excellent theoretical support has been provided in producing these results, but more extensive collaboration between experimenters and theorists will be needed for the great potential of this vital program to be fully realized. DESY is one example of such a collaboration. Through an active series of workshops and with the help of theorists at DESY, experimenters have found broad and effective support from theorists in Europe and in the US. To foster activity on a similar scale within the US program, a renewed commitment to QCD studies should be made at the same level. Elsewhere in the US, the QCD programs at both SLC/SLD and CLEO/CESR have produced significant results and promise to continue to do so. A QCD program at the NLC would offer an opportunity to make further precision tests. Finally, important US efforts exist that participate in the European QCD programs at HERA and LEP. In addition, the new window on QCD physics to be opened up by the energy regime at the LHC should produce a rich program of QCD measurements. US involvement in these European programs is vital to keeping US physicists engaged at this QCD frontier. Of primary importance, however, remains the need for leadership in the maintenance and expansion of QCD experiment and theory in the US.

3 Experimental Studies of QCD

3.1 Introduction

The experimental study of QCD has evolved considerably since the last decade when the principal goal was to "test QCD" to the present activity of measuring QCD elements such as α_S, fragmentation, and parton distribution functions. Present tests of QCD explore the frontiers of the theory, such as the boundary between perturbative and non-perturbative QCD of small-x and diffractive phenomena. The experiments of the future will provide precise measurements of QCD that will significantly enhance our knowledge of strong interactions and should aid in the discovery of the Higgs and the detection of deviations from the standard model such as composite quarks. Future experiments to explore the quark-gluon plasma will also open a new area of QCD exploration.

3.2 Measurements of α_S

The measurement of α_S for a variety of processes and Q^2 scales provides a fundamental test of QCD. The most precise direct measurement of α_S to date has been made by the LEP experiments for $Q^2 = M_Z^2$[1]. SLD has also produced comprehensive results on measurements of α_S from jet rates, energy-energy correlations and event shapes[2]. A summary of these results is shown in Figure 1. SLD and LEP results also provide evidence for the flavor independence of α_S. Ultimately, it is hoped to obtain a precision approaching a couple of percent for the α_S value measured for each quark flavor. Measurements of α_S will also be pursued with high priority at LEP 2, using jet rates, energy correlations and event shape variables such as thrust. The large lever arm in c.m. energy provided by an NLC and the reduced uncertainty due to hadronization effects should allow determination of α_S to about 4% and tests its running with energy[3].

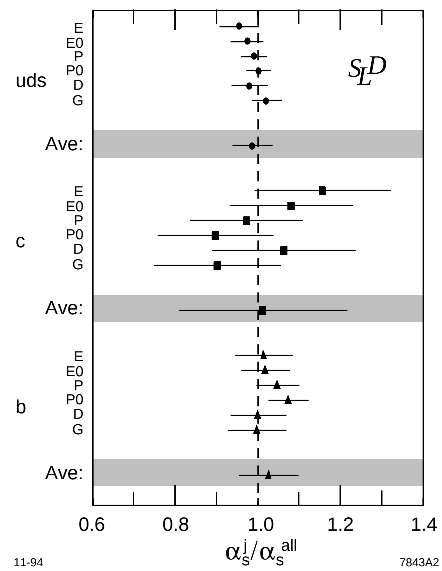

Figure 1: SLD Measurements of α_S and its flavor dependence.

The CCFR (FNAL E770)[4] νN scattering value of α_S measured from xF_3 and F_2 at high x is in good agreement with results from E-665 as well as the CERN NMC and EMC μN scattering experiments and other deep inelastic and low energy measurements. However, the low energy measurements are systematically slightly different from the LEP results. This difference may be due to the QCD scale value and definition in terms of renormalization scheme as well as higher order corrections. The forthcoming νN experiment, NuTeV (FNAL 815), expects a factor of 2 improvement in the statistical error on α_S, along with improvement on systematics, which could increase the significance of this difference.

Hadron collider measurements of α_S can be obtained by comparing ratios of cross sections $\sigma(X + (n + 1)\,\text{jets})/\sigma(X + n\,\text{jets})$ where $X = \gamma$, W, Z, or jet. For example, DØ[5] has performed a measurement of α_S from $W + 1\ jet/W + 0\ jet$. Hadron collider measurements will complement the LEP results, test the process independence and flavor independence of α_S, and provide measurements of the running of α_S over a large Q^2 range.

HERA measures α_S from deep inelastic scattering and the evolution of the structure functions. The experiments ZEUS and H1 measure deep inelastic scattering over a large range of Q^2 from a fraction of a GeV^2 to 10^5 and x below 10^{-4}. HERA also measures the relative rate for 2 jet events (+ the proton remnant) to 1 jet events which is sensitive to α_S. At HERA, this measurement can be performed for different values of Q^2, so that it may be possible to see the evolution of α_S within one experiment over a large range of Q^2.

The running of α_S over a large range of Q^2 is also shown by the dijet angular distributions from CDF[6] and DØ[7]. This range will be greatly extended at the LHC.

3.3 Parton Distributions and Structure Functions

The HERA *ep* collider has greatly extended the range of x and Q^2 accessible for experimental measurement beyond that of the previous fixed target experiments. This is shown in figure 2. The HERA measurements[8] show a rapid rise in F_2 as x decreases at low x (x values down to $\approx 10^{-4}$ were probed.) The conclusion is that the data prefer a rising gluon density leading to a rising sea quark density as x decreases. New data from H1 and ZEUS indicate that the rise at fixed Q^2 at low x appears to be softer for lower Q^2. The x region accessed by HERA is important since existing structure function parametrizations are checked with data only down to $x \approx 0.04$. HERA is now providing knowledge about the gluon distribution at low x. The HERA measurements will be considerably refined in the next few years as luminosity increases and the detectors are better understood. Already, preliminary measurements down to $Q^2 = 4.5$ GeV^2 have been presented. Upgrades and special running conditions (shifted vertex, lower energies) should provide the measurements to extend to Q^2 below 1 GeV^2. This will allow detailed tests of the scaling behavior of QCD via $dF_2/d\ln Q^2$, as well as the refined extraction of the gluon density. Data from electron and positron beams in principle allows a measurement of the non-singlet valence distribution, $F_3(x, Q^2)$, limited only by HERA statistics. An extraction of F_L will be possible, which provides information about the gluon density, along with F_2. The gluon structure function can also be measured via the boson-gluon fusion rate and other independent ways at HERA.

So far, the main tools in studying small-x behavior have been the Balitsky, Fadin, Kuraev, Lipatov (BFKL)[9] and Dokshitzer, Gribov, Lipatov, Altarelli, Parisi (DGLAP)[10] equations. These equations generate the leading growths at small x in different kinematical regimes. At present there is an intense activity to decide which of these mechanisms is responsible for the small-x behavior seen at HERA.

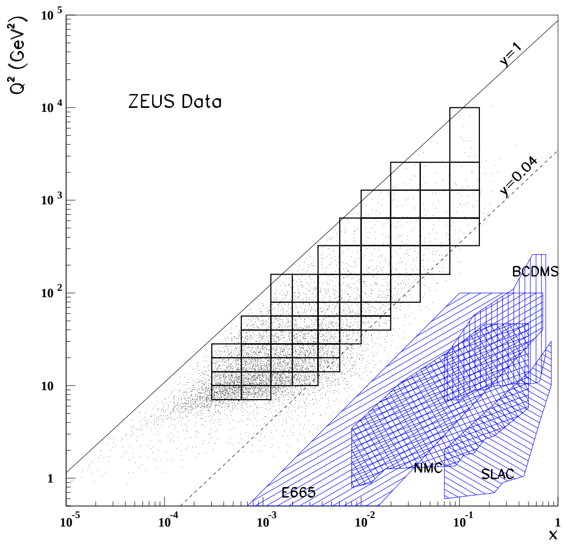

Figure 2: ZEUS 1993 data with the bins used for structure function analysis compared with the range of coverage of fixed target experiments.

Hadron collider measurement involve the convolution of two parton distribution functions. As the accuracy of the perturbative QCD predictions improves, these measurements can also reliably be incorporated into the global fitting programs used to extract parton distributions. Consistency of the extracted distributions amongst the various experiments is in itself a QCD test, and checks the factorization hypothesis. The kinematic range of the Tevatron collider is $2 \times 10^{-3} \lesssim x \lesssim 1$ and 10^2 GeV$^2 \lesssim Q^2 \lesssim 10^5$ GeV^2. CDF data provide measurements of the gluon, sea-quark and heavy flavor parton distributions in the proton, and yield constraints on flavor asymmetries in the quark distributions. Jet and γ production are sensitive to the gluon distribution. Drell-Yan production can be used to constrain the sea-quark distributions. $W + c$ and $\gamma + c$ production provide direct measurements of the strange and charm content of the proton. In addition, measurements of the asymmetry in W production are sensitive to the u/d ratio.

CDF[11] and DØ[12] are studying the triple differential cross section $d^3\sigma/dE_t d\eta_1 d\eta_2$. The result from DØ is shown in Figure 3. This can be directly mapped to the x_1 and x_2 of scattering partons and measuring this truly triple differential gives information of parton distributions between: $x = 0.003$ and 0.7 or higher. It is hoped that the new hadron collider data will extend the results to x as low as .001. Data from the LHC will probe to much lower x. The triple differential cross section is also a direct measure of the gluon content of the proton since at low p_t all scattering occurs through gluon-gluon scattering. However, understanding of the results awaits further NLO predictions.

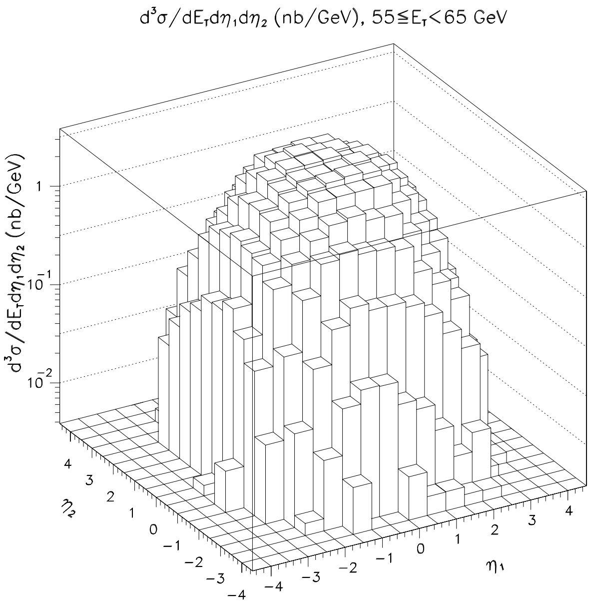

Figure 3: The triple differential cross section $d^3\sigma/dE_t d\eta_1 d\eta_2$ from DØ

In fixed target μN scattering, FNAL E665 has new measurements of the structure functions F_2^p and F_2^N in new regions of x and Q^2 as well as a measurement of σ_n/σ_p down to x of 10^{-3}. Comparison of F_2 in μ and ν scattering shows disagreement at low x[13,14]. The discrepancy is in x bins measured by only single experiments – CCFR (ν) and NMC (μ). New, higher precision results in both ν and μ will help address this problem. Through measurement of opposite sign dimuons, νN scattering also determines the strange sea and NuTeV should improve these measurements.

3.4 Spin Structure Functions

3.4.1 Background

In 1988, the EMC μN scattering experiment[15] presented a measurement of the nucleon spin structure function that violated a sum rule developed by Ellis and Jaffe[16]. The interpretation of the sum rule violation was that the strange sea in the proton is highly polarized. Another interpretation of the measurement was that the valence quarks carry little spin, the remainder carried either by the gluons or by orbital angular momentum. Experimental programs at CERN, at SLAC, and more recently at DESY were launched to explore this. The SLAC experimental program consists of four experiments (E142, E143, E154, E155) aimed at studying the proton and neutron spin structure in detail. SLAC experiment E142 ran in 1992 and found small negative asymmetries in the scattering of polarized electrons off polarized neutrons in the ^{3}He nucleus[17]. In parallel, the SMC program at CERN looked at the scattering from polarized deuteron targets[18]. These experiments address the significant questions concerning the fraction of the nucleon spin carried by the quarks and the strange sea polarization in the neutron spin structure function[19]. The combined neutron and proton results allow for a test of a fundamental QCD sum rule developed by Bjorken[20].

3.4.2 Recent Developments & Future Outlook

Recently, SLAC Experiment E143 used polarized ammonia and deuterated ammonia targets to remeasure both the proton and deuteron spin structure functions to high precision. The electron beam polarization and energy were improved to 80% and 29 GeV. Most recently, in 1994, E143 at SLAC[21] and SMC at CERN[18] reported new data on polarized protons. Latest indications are that between 30% to 40% of the proton's spin is carried by the bare valence quarks. This still seems somewhat less than might have been expected from predictions based on constituent quark models of the nucleon. It has been suggested that this result signals a breakdown of the quark model and possibly an indication that some aspects of the nucleon are better described by a chiral (Skyrme) model[22]. It has also been noted that the flavor singlet axial anomaly complicates the traditional interpretation of the first moment of the g_1 structure function in terms of the quark spin in the proton[23]. A good measurement of the distribution of gluon spin in the nucleon would be likely to give strong support to one or the other of these suggestions. The issues here are very important. The reliability of the quark model, and the viability of Skyrme-type models will rest on determining just which partons carry how much of the nucleon's spin.

In the future we can expect data from two more experiments at SLAC which have been approved to use a higher energy 50 GeV beam. With this higher energy, lower x and higher average Q^2 measurements of the spin structure functions will be measured. The total combined data set from these SLAC experiments alone should be adequate to test the Bjorken sum rule to better than 10% of its value. The forthcoming HERMES experiment at DESY will also provide a precise determination of the g_1 sum rules for the proton and neutron. The resulting uncertainty in the Bjorken sum rule is expected to be 5-8%. HERMES will also determine the g_2 structure function (associated with transverse target polarization) for both the proton and neutron. This structure function allows the first direct study of quark- gluon correlation functions without contamination by leading twist-2 structure functions. HERMES will carry out measurements of coincident hadrons produced in spin-dependent deep inelastic scattering. These measurements will provide information on the flavor dependence of the polarized structure functions as well as the contribution of orbital angular momentum. In addition, these measurements are expected to be sensitive to $h_1(x)$, the chiral-odd leading-twist structure function.

3.4.3 Polarized Proton Physics

The polarized beam capability proposed for RHIC offers a unique array of spin measurements[24]. This allows the measurement of $g(x)$ for nuclei, $\Delta g(x)$ for pN, $h_1(x)$ (which counts the valence quark polarization), parity violating terms in W and Z production and the sea quark helicity difference in W production. The Drell-Yan process can also be used to measure spin observables with longitudinal and transverse polarization to yield new information about antiquark and valence quark polarization. Gluon polarization can be measured by using direct photons from the dominant quark-gluon Compton graph and through medium p_t jets (20 - 50 GeV/c) which are predominantly quark-gluon produced. Parity violation in W^+ production measures the difference between u and $\bar{d}$ polarization, and for W^- production it measures the difference between d and $\bar{u}$ polarization. h_1 will be measured with transverse spin using both γ^* and Z production. Experiments at RHIC should also be able to search for parity violation in other processes (jets, γ).

3.5 Tests of Perturbative QCD

3.5.1 Jets and Final States

CDF and DØ have produced a wealth of data on jets and final states. DØ has compared the overall inclusive cross section, $d^2\sigma/dE_t d\eta$, jet and dijet cross sections, and direct predictions[5]. They have uniform rapidity coverage for $-4.0 < \eta < 4.0$ and can extend the coverage for jets down to transverse energies (E_t) of 15 GeV. They observe that jet cross sections measured out to $\eta = 3.0$ agree within errors with NLO predictions over more than 10 orders of magnitude. DØ has measured the dijet angular distribution over an extended range, which tests the correctness of LO and NLO hard parton cross sections. DØ has compared the location of a third jet in an event with respect to the second leading jet ordered by E_t and see an enhancement predicted by color coherence.

CDF also observes color coherence effects in hadronic angular ordering which provides evidence for the interference between the initial and final state gluon emission from color connected partons. CDF has compared the inclusive jet E_t spectrum, the two-jet mass spectrum and angular distribution, and the two-jet differential cross section with the NLO predictions[6,25]. There is good agreement between the measured and predicted differential cross sections. These NLO comparisons agree at the $\pm$ 20% level, which is about a factor of two better than the precision of the corresponding comparisons at LO. In the future, a combination of improved theoretical calculations and data from luminosities between 100 pb^{-1} and 1 fb^{-1} should result in QCD measurements with a precision of a few percent.

Not all the current CDF measurements show good agreement with QCD predictions. There are significant discrepancies between the data and NLO theory for the ratio of scaled inclusive jet cross sections measured at two values of $\sqrt{s}$ (1800 GeV and 546 GeV)[26] and the inclusive photon spectrum at low p_t[27]. While the newer measurement of the b production cross section by CDF[28] appears closer to the QCD prediction than previous measurements[29], the b cross section measurement by DØ[30] agrees with QCD expectations. At LO there are order of magnitude discrepancies with the measured prompt ψ and ψ' production cross sections. The resolution of these discrepancies is clearly important to establish the reliability of the QCD predictions and may lead to some new insights.

The new kinematic regime available at the Tevatron should provide a test of QCD calculations in the semi-hard region. As dijet separations reach large rapidities a second scale, $\ln(s/p_t^2)$, enters the perturbative expansion, leading naturally to a resummation in terms of the BFKL Pomeron[31]. It will be one of the exciting challenges, over the next five to ten years, to make precise comparisons between theory and experiment and to measure the BFKL Pomeron. Already some data on rapidity gaps at FNAL energies had appeared[32,33].

Numerous tests of perturbative calculations have been performed at SLD and LEP 1. These include tests of second order formulae (for quantities like thrust, oblateness and other event shape variables) and resummed calculations[34]. Most of these studies will be repeated at LEP 2, where the reduced theoretical and hadronization uncertainties will make the comparisons of theory and data even more unambiguous. There are still relatively few variables for which resummed calculations have been performed. New calculations utilizing perturbation theory beyond second order will be tested at SLD, LEP 1 and LEP 2, as they become available. Tests of perturbative calculations relevant for coherence phenomena, the interference effects associated with the coherent emission of soft gluons, have been performed at LEP 1 and will be continued. Studies of coherence should benefit from the smaller hadronization uncertainties at LEP 2.

Tests of matrix elements at LEP comprise measurements of the absolute and relative energies and angles of jets in three-, four- and five-jet events and a comparison to matrix element formulae[35]. Investigations of the three-jet matrix element at LEP have yielded much more rigorous tests than were possible at PETRA and PEP, because the jet resolution parameter (y_{cut}) can be made much smaller: this means that the pole structure arising from soft gluon radiation can be observed and compared to theory. Also, it is possible to study the matrix elements at much smaller scaled jet energy values, x.

The properties of quark and gluon jets have been studied at LEP, using tagged quark jets and rare, two-fold symmetric three-jet events to obtain unambiguous results on quark and gluon jet differences[35]. These investigations, which require large data statistics, will continue to the end of the LEP 1 program.

CLEO is performing a QCD analysis of jet rates in e^+e^- 4-flavor continuum around 10 GeV to study if there is a difference between the 4-flavor and 5-flavor cross sections due to flavor dependence [36].

Studies are underway to determine whether perturbative QCD is able to describe deep inelastic scattering jet data, both in the FNAL E665 [37] kinematic regime and in the high-energy regime of HERA[38,39]. QCD models of final state radiation have been well tested at other accelerators, such as LEP. However, the initial state radiation predictions are not well tested. HERA offers the opportunity to perform such tests.

Initial data from HERA indicates that deep inelastic scattering two-jet data are dominated by QCD Compton and boson-gluon-fusion processes. The overall energy flow in deep inelastic scattering events should manifest the filling of the phase space between the current jet and photon remnant with particles materializing from the emission of additional gluons and quarks created by color transfer between the struck quark and proton remnant. Effects such as color coherence are being studied. Several QCD models tested by these data are found to agree. As the increased statistics from HERA become available, there will be an iterative process as QCD models are refined to agree with more precise data. A measurement of the gluon density from jets should be available within about a year.

Jet production in deep inelastic scattering with $Q^2 > 4$ GeV^2 has been investigated at HERA for events with center-of-mass energies W between 30 and 280 GeV[38,39]. The characteristics of the multijet events are not consistent with a bare quark-parton model, but are well described by the first order QCD matrix elements plus higher order corrections implemented via parton showers. Multijet production has also been studied in events with a large rapidity gap. The properties of these events with $W > 140$ GeV are consistent with a leading twist diffractive production mechanism. These analyses indicate that considerable information may be gleaned from inelastic and diffractive jet production at HERA. Studies at HERA of multijet production and differential cross sections in quasi-real photoproduction at center-of-mass energies in the range 130 - 275 GeV have been compared with leading logarithm and parton shower predictions, including resolved and direct processes. Future data should allow a determination of the photon structure function via photoproduction of jets.

Jets in lepton-hadron interactions have also been observed in FNAL experiment E665[37]. They have measured 2 + 1 jet rates corrected to the partonic level, and compared these with LO and NLO calculations, which they find underestimate the data. They are also analyzing the propagation of multijets in nuclear matter using nuclear targets. They expect to analyze a sample 30 times larger in the next 2 years. Increases in fixed target energy, however, cannot match the kinematic range at HERA, which is the equivalent of a 52 TeV electron beam on a fixed proton target.

3.5.2 Photoproduction

The next few years should see detailed measurements of the photon structure function at HERA from photoproduction events ($Q^2 \approx 0$). Besides $p\bar{p}$, γp scattering is the only other hadronic interaction which can be currently measured at c.m. energies above 100 GeV. As is the case for purely hadronic interactions, photoproduction has a soft component due to peripheral processes and a hard component due to the scattering of a parton in the proton with a parton in the vector meson from the photon. However, the photon also has a direct pointlike coupling to quarks that leads to additional hard scattering processes that are not present in hadron-hadron interactions. "Direct" processes include the photon-gluon fusion into a quark-antiquark pair and the photon scattering off a quark in the proton with the emission of a gluon (QCD Compton scattering). These processes are also measured in direct photon production (see Section 3.5.4). "Resolved" processes include the hard scattering of the hadronic (vector meson) photon, and the hard scattering due to the quark and gluon content of the photon. Studies of these processes at HERA over the next few years will result in a detailed measurements of the hadronic structure of the photon and the gluon distribution of the proton.

Other interesting processes that can be studied at HERA with photoproduction events include boson gluon fusion producing heavy quarks, such as in J/ψ production. These processes will also help measure the gluon distribution of the proton. In general, the hadronic properties of the photon will be studied in great detail. Already, the direct and resolved scattering of the photon on the proton have been observed. In addition, the observation of hard scattering photoproduction events with rapidity gaps offers the opportunity to measure the elastic and inelastic diffractive contribution. Two-jet production in hard-scattering photoproduction events will allow determination of the photon structure function.

Measurements of the photon structure function, $F_2^\gamma(x, Q^2)$, in the two-photon reaction $e^+e^- \to e^+e^- + hadrons$ have been performed at LEP 1[40]. This topic will be pursued actively at LEP 2 and will allow an investigation of the scaling behavior of $F_2^\gamma(x, Q^2)$ over a large Q^2 range.

3.5.3 Heavy Quarks

Heavy quark experimental results have some unresolved QCD issues. As mentioned above, there is a disparity between the NLO QCD calculation of the b cross section and experimental data from UA1 and CDF. However, the new DØ cross section results are in good agreement with theory. These results have been compared to heavy quark predictions and are sensitive to gluon density in their normalization and rapidity dependence. The transverse momentum (p_t) distribution of B mesons rises faster than predicted by NLO calculations. In Tevatron fixed target experiments, there is a deviation between the angular distributions of back to back peaking of charm and beauty particles and NLO QCD predictions, although the b-particle statistics are limited[41]. Higher energy fixed target experiments would permit sufficiently precise measurements for b-particles.

The measured Feynman x-distributions of J/ψ and other charmed hadrons present an important challenge for QCD theory and phenomenology. Such distributions, especially at large values of x, are very sensitive to higher twist effects. Understanding the nuclear A-dependence and large-x dependence of J/ψ production may also have important consequences for the use of J/ψ production as a signal for the quark-gluon plasma formation in heavy ion collisions. At the moment there is no general consensus as to what physics determines the large-x behavior of heavy particle production. However, progress is being made by both nuclear and particle theorists, which should hopefully lead to a satisfactory understanding of this area in the future.

3.5.4 Single Photons

DØ has measured the direct photon cross section in the central region[42], and will extend this in the next year to the $\eta > 1.0$ region. This is used to measure the gluon density of the proton. CDF finds a 20% discrepancy with QCD predictions for the single photons with $p_t \lesssim 30$ GeV[43]. This discrepancy could be due to inadequate knowledge of the gluon distribution in the x range probed or to photon fragmentation. Better measurements of these phenomena should help to resolve this.

LEP 1 can study photon radiation from quarks since the Z^0 pole suppresses initial-state photon radiation[44]. So far, QCD studies of final-state photon radiation have concentrated on isolated, high-energy photons in order to test the parton shower mechanism, since photons are emitted according to a matrix element similar to that for gluons, without the complications of hadronization. These studies will continue to the end of the LEP 1 program. Studies of final-state photon radiation *within* jets have now begun, with the purpose of measuring the quark to photon fragmentation function.

3.5.5 Other Tests of Perturbative QCD

The SLD experiment plans to exploit particle identification, secondary vertex identification and polarization to explore QCD quark/antiquark and flavor dependence. They have compared multiplicities of events with b- and uds- tags[45]. They will focus on the charm sector where tests of perturbative QCD can be made at the c-mass, close to the confinement scale. SLD also plans to compare gluon radiation patterns from heavy and light quarks. They are studying parton polarization in hadronic jets.

CLEO is comparing semihard reactions in two-photon collisions, *e.g.*, $\gamma\gamma \to$ V+X, with calculations in perturbative QCD. They will also continue tests of QCD predictions for $\gamma\gamma \to \pi^+\pi^-, p\bar{p}$ as well as $\Upsilon \to gg\gamma$, and the two-photon decay widths of the η_c and χ_{c2}[46]. CLEO also intends to test some of the predictions of the modified leading log approximation and local parton hadron duality for multiplicity differences between charm quark and light quark events.

Resummed QCD predictions for the W and Z p_t spectrum have been tested with CDF data and found to be in good agreement[47]. The Drell-Yan cross section makes an ideal measurement for a systematic comparison between NLO, NNLO and resummed QCD. CDF expects to measure this within 5-10% from their present data. DØ also uses the p_t spectrum of the Z to test QCD techniques employed in calculations, including, resummation and NLO high p_t predictions[48]. DØ has examined the energy flow in W and jet events and shown that there is a difference between the energy flow around a colored versus a colorless object, as predicted by QCD.

3.6 Boundary between Perturbative and Non-Perturbative QCD

There are many examples where collider data give information on phenomena at the boundary between perturbative and nonperturbative QCD. Examples include the onset of small x effects, and the study of the hard diffractive process and rapidity gap events.

3.6.1 Small-x

As smaller values of x are probed for a fixed Q^2, the density of partons is predicted to increase. The approximations made in deriving the perturbative evolution equations (leading $\ln Q^2$) are no longer valid. The opportunity to explore the small-x region at HERA has generated much interest. For example, for $Q^2 = 10$ GeV^2, x values as small as 10^{-4} can be reached at HERA. Early data from HERA indicate that the parton distributions are rising quickly, and are close to the predicted $x^{-0.5}$ behavior[49]. This rapid increase in the parton density would eventually lead to a violation of unitarity. This implies that a saturation of the parton densities will occur below some value of x. Searches for this saturation are an important part of the tests of QCD at HERA. The data from H1 and ZEUS will also indicate how large the gluon densities become, if there is gluon recombination, if partons overlap and whether there are "hot spots"[50].

While CDF and DØ have begun to study small-x effects, their analysis would be enhanced by increasing kinematic coverage of jet and photon measurements and improving their detector understanding. However, more theoretical input is also needed to understand the types and magnitude of phenomena to be expected. For instance, it is possible to look for small-x effects in jet events with large rapidity gaps. Both DØ and CDF have investigated these effects[32,33], although the theoretical framework here also needs better understanding.

3.6.2 Diffractive Scattering & Rapidity Gaps

The observation at HERA of deep inelastic scattering events with a large rapidity gap in the final state between the proton direction and the first energy deposit in the detector is an indication of diffractive scattering[51]. The flatness of the rapidity gap distribution, as well as other properties of the events such as independence of the cross section on W, are consistent with photon diffractive dissociation off a Pomeron. A detailed study of these events may yield insight into the transition from perturbative to non-perturbative scattering. Exclusive reactions, such as elastic vector meson production, should provide stringent tests of calculations in perturbative QCD, as well as new methods for extracting gluon distributions. Finally, if the Pomeron has small dimensions compared to the proton, then new low-x effects such as saturation would set in even earlier. The two HERA experiments will upgrade their detectors in order to measure the scattered particle in these events and allow a precise measurement of the kinematics of the final state. This will enable measurements of the Pomeron structure function as well as measurements of the structure function of virtual pions.

Rapidity gaps have been found at the Tevatron[32,33] and are now a subject of considerable interest. In principle, such events are an excellent place to study high-energy semi-hard physics including the BFKL Pomeron. However, the analysis is complicated by the presence of hadrons coming from soft interactions involving the spectator quarks in the colliding hadrons. More experimental work, such as a comprehensive search for rapidity gaps in various channels, is essential. More theoretical work is necessary in order to make sharp contact between QCD theory and experiment. This promises to be an interesting subject in the coming years.

Diffractive physics at the LHC promises to be a rich source of information since certain topologies will be cleaner. due to cleaner events. It will be possible to look for diffractive Higgs events with reduced hadronic activity in the rapidity region near the Higgs particle[52]. Both single and double pomeron exchange can be observed, particularly in $H \to \gamma\gamma$ events. In addition, single diffraction at the LHC can be studied in $b\bar{b}$ production.

3.6.3 Jet Fragmentation

CDF has made comparisons of the average jet shape (energy flow inside jets) with NLO two-jet predictions that show good agreement[25], indicating that there is a perturbative piece of jet fragmentation that can be calculated. In the future, the scope of the QCD measurements will widen to include more detail on jet shapes, fragmentation, energy flow in the "underlying event" accompanying hard processes and the energy flow in rapidity gap events. CDF also has the capability of measuring the fragmentation of heavy flavor jets, the fragmentation of generic jets to γ's and π^0's, and differences between quark jets and gluon jets. DØ has measured the E_t profile of jets as a function of the distance from the jet axis for different E_t's and rapidities[5]. Clear differences are observed and in general the behavior is described well by the parton shower model.

The CDF and DØ studies complement the information from the LEP and SLC experiments and provide checks of the universality of jet fragmentation. The large statistics of the LEP 1 experiments permit a substantial number of heavy resonance states to be reconstructed and their production characteristics and correlations to be studied[44]. These studies will include such topics as baryon creation from the vacuum. SLD plans to measure heavy quark fragmentation functions and decay topologies and study particle fragmentation properties separately in quark and antiquark jets.

3.6.4 pp and $\bar{p}p$ Elastic Scattering

At Fermilab there is a program of measuring $\bar{p}p$ elastic scattering up to $\sqrt{s}$ range $0.6 - 2$ TeV. At RHIC, there will be a systematic study of the proton-proton elastic scattering in the $\sqrt{s}$ range $60 - 500$ GeV and covering the four-momentum transferred $|t|$ up to 8 (GeV/c)^2. The small $|t|$, or Coulomb nuclear interference region, determines the total cross section, the ratio of real to imaginary part of the scattering amplitude, and the slope parameter. These measurements should clarify some of the present puzzles connected with elastic scattering[53].

At large $|t|$, where data can be taken with the standard lattice, $|t|$ values beyond the expected second dip can be reached. At these $|t|$ values it is possible to make a comparison with perturbative QCD calculations. The same setup can be used to study elastic scattering using polarized protons at RHIC, to measure the difference in the total cross sections as function of initial transverse spin, the analyzing power, and the transverse spin correlation parameter. At lower energies, the spin dependence in polarized proton-proton elastic scattering has a very strong angular dependence which has never received satisfactory explanation. It will be interesting to see whether the strong t-dependence of A_{NN} persists at higher energies.

3.7 Quark Substructure

Quark substructure is investigated by measurement of the inclusive jet cross section. Composite quarks would manifest themselves through deviations from the standard QCD expectations at high transverse momenta where valence quark scattering dominates. The present CDF limit on the compositeness scale is $\Lambda_c > 1.4$ TeV (95% C.L.). By the end of the decade the expected two orders of magnitude in statistics and increase in energy from 1.8 TeV to 2.0 TeV should improve this limit to 1.8 TeV. LHC exposures of 10^4 and 10^5 pb^{-1} would result in sufficient statistics to observe a compositeness scale Λ_c as large as 15 and 20 TeV, respectively. The largest systematic error is expected to be that caused by a nonlinear performance of the calorimeter. The anticipated performance of the ATLAS and CMS detector calorimeters should be adequate to explore the compositeness scale out to the 15 - 20 TeV range.

3.8 Light Hadron Spectroscopy

3.8.1 Light Quark Spectroscopy

A thorough understanding of the conventional $q\bar{q}$ nonets is an important area in which to look for extraneous states, or states with peculiar production or decay characteristics. Exotic J^{PC} combinations can also be looked for. Some of the processes used in these studies include peripheral production, peripheral production which emphasize OZI-disallowed processes, central production, $p\bar{p}$ annihilation, J/ψ radiative decays and photon-photon scattering. Brookhaven experiment E852 will collect a substantial sample of final states with charged particles and neutrals. This should address the issue of the only reported exotic to date, the $J^{PC} = 1^{-+}$ M(1405)[54], since E852 will be sensitive to many more modes and able to search for the exotic hybrid which should decay into b1(1235) π, as well as investigating $\eta - \eta$, $\eta - \eta'$ and various vector-vector states.

3.8.2 Glueballs

Glueballs are a direct consequence of the non-abelian nature of color $SU(3)$ and so their observation would be an important demonstration of non-perturbative QCD in hadron spectroscopy[55]. They are the only unobserved hadrons predicted by $SU(3)$, but there is no consensus on whether they exist. Lattice gauge theory (see Section 6.2.2) predicts the lowest lying glueball states to be a 0^{++} state with mass $\approx 1740 \pm 71$ MeV and a 2^{++} with mass $\approx 2359 \pm 128$ MeV. In the case of the 0^{++} the number of isoscalars found so far are 4 [$f_0(975)$, $f_0(1400)$, $f_0(1590)$, $f_0(1720)$], only one of which is expected to be a $q\bar{q}$ state. Thus, at least two must be eliminated to have a possible candidate for a 0^{++} glueball. Multiquark, quark molecule, or hybrid states are all candidates for these other states[56], which adds to the uncertainty.

In the 2^{++} channel the reaction $\pi^- p \to \phi\phi n$ at BNL revealed a breakdown of the OZI suppression and later the existence of three candidate ($\phi\phi$) glueball states, the $f_2(2010)$, $f_2(2300)$ and $f_2(2340)$, with classic Argand diagrams. The many Godfrey-Isgur $q\bar{q}$, and multiquark states expected in this region were not observed, suggesting that these 2^{++} glueball candidates break the OZI suppression. In the next year or two, runs are expected in Brookhaven experiment E-881 to enhance non pion exchange processes. By studying $K^- p \to \phi\phi\binom{\Lambda}{\Sigma}$ (OZI allowed) and $\bar{p}p \to \phi\phi\pi^0$ (OZI forbidden) one hopes to further clarify the situation.

3.9 Quark-Gluon Plasma

3.9.1 RHIC Program

The Relativistic Heavy Ion Collider (RHIC) and the PHENIX, STAR and PHOBOS detectors are designed to study the reorganization of matter predicted to occur in high-energy nucleus-nucleus collisions. These collisions range from Au + Au at $\sqrt{s}$ of $60 - 200$ GeV per NN pair at a design luminosity of 2×10^{26} to pp at $\sqrt{s}$ of $50 - 500$ GeV at a design luminosity of 10^{31}, with the option to provide longitudinal and transverse polarized beams. The large systems of highly excited, strongly interacting matter formed in these collisions will be probed to search for signatures of the existence of the quark-gluon plasma - a state of matter in which quarks and gluons are 'deconfined' and where chiral symmetry is restored. QCD issues that are addressed by this program are to establish the existence of a quark-gluon phase of matter and measure the properties of matter in the region of the phase change. Also to be studied are nuclear shadowing and color transparency. The program is scheduled to start in 1999.

The detectors at RHIC should address almost all aspects of quark-gluon plasma formation and chiral symmetry restoration in nuclear collisions. The early stages of the collision, expected to be a gluon-dominated QCD plasma, can be studied in PHENIX using electromagnetic probes (lepton-pairs and photons). Alternatively, one can look for open charm through the decays $D \to$ leptons in PHENIX and potentially $D \to$ charged hadrons in STAR. The quark-gluon plasma phase will be investigated by measurements of predicted signatures, such as suppression of heavy vector mesons $(J/\Psi, \Psi, \Upsilon)$ through μ and e-pairs measurements in PHENIX. Similarly, it is planned to search for the enhancement of strangeness production using strange hadron measurements in STAR and PHENIX and multiple-strange baryons and antibaryons in STAR.

If the QGP phase transition is first-order, a dramatic increase in the differential source size is expected due to the time-delay associated with particle emission accompanying a first-order phase transition. Such behavior can be inferred from two-particle interferometry measurements in PHENIX, PHOBOS and STAR. The characteristic phase transition behavior of the temperature as a function of entropy density in this case can be measured in STAR and PHENIX; and local density fluctuations in particle number, energy, and entropy could be observed in STAR and PHOBOS. Direct photons from the mixed phase will be measured by PHENIX. Measurements of the mass, width and yield of ϕ-mesons via $\phi \to e^+e^-$ in PHENIX and $\phi \to K^+K^-$ in PHENIX and STAR could detect possible modifications of particle masses and widths in the medium due to partial chiral symmetry restoration.

Localized regions of disoriented chiral condensate, formed in the chiral phase transition, expected to be second-order, could be measured in STAR, via abnormal ratios of the various charges of pions in localized regions of momentum space event by event.

To be able to understand RHIC collisions and perform reliable perturbative QCD calculations, the initial conditions of the collision must be well understood. This requires measurements of the gluon structure function and nuclear shadowing of quarks and gluons in the x region $0.02 < x < 0.1$. These measurements can be done directly at RHIC. The process gluon + quark $\to \gamma$ + jet will be measured in STAR to determine the gluon structure function. Both STAR and PHENIX, through γ + jet coincidences and direct γ measurements, respectively, can determine the degree of nuclear shadowing.

3.9.2 LHC Program

The LHC heavy ion program will involve a dedicated detector, ALICE, as well as operation of the two general purpose pp collider detectors, ATLAS and CMS. These experiments will study the production of heavy quarkonium states ($c\bar{c}$ and $b\bar{b}$) to look for signs of quark-gluon plasma. These studies will concentrate on bottomonium production rather than charmonium since J/ψ production from B-meson decay dominates at the LHC, except at very low p_t. These detectors will study the global event characteristics as a function of energy density and also examine the suppression of Υ' and Υ'' with respect to Υ production. At the LHC with 10^5 Υ, corresponding to an integrated luminosity of 15 nb^{-1}, the estimated precision of the measurement of the suppression is 7 (20)% for the Υ' (Υ'')[57].

3.10 Conclusions

Many areas of QCD experimentation are producing new and important results. There is new information on parton distribution functions, QCD parameters and tests of consistency between perturbative QCD and data. Quantitative collider measurements are yielding new insights in processes such as Drell-Yan production, jets, direct photon production and heavy quark production. The frontier of our knowledge of QCD is being explored in studies of large transverse momentum processes, small-x scattering, diffractive processes and rapidity gaps. Finally, we are just beginning to explore areas of exclusive reactions, spin physics and QCD in nuclei.

The wealth of new and more precise QCD measurements presents an important opportunity to enhance our understanding of the strong interaction and the structure of the nucleon. However, the sophistication of QCD theory beyond the parton model and the complexity of modern experiments requires much more close collaboration between theorists and experimentalists. Efforts such as that of CTEQ (Collaboration between Theorists and Experimentalists on QCD) are particularly important to provide this and should be broadened.

There are many open questions to be explored in QCD. These include the gluon distribution, the flavor-dependence of the sea, features of direct photon production and jet differential cross sections, heavy quark production, the small x region, diffractive phenomena, spin physics and the quark-gluon plasma. QCD represents an extraordinarily rich area for continued theoretical and experimental exploration. The confrontation of QCD theory with improved experiments will produce insight on the structure of hadrons, understanding of the underlying quantum field theory and clues that may point to new physics.

4 Theoretical Studies of QCD

4.1 Factorization in Processes with a Hard Scattering

There are a few processes, such as $\sigma(e^+e^- \to hadrons)$ at high energies and , $(Z \to hadrons)$, where perturbative QCD gives a complete description of an observable. However, in the general situation where hadrons make up one or both of the initial particles in a scattering, or when a hadron with some definite momentum is measured in the final state, nonperturbative effects are important. Factorization in a high-energy hadronic reaction, which at the same time has a hard scattering, gives the cross section for that process as a product of a perturbative hard scattering cross section of quarks and gluons times parton distributions in the initial hadrons[58,59]. These parton distributions give the flux of quarks and gluons available for the hard scattering. They are universal, depending only on the hadron from which they come but not on the particular hard process. Thus the quark and gluon distributions in the proton can be determined, say, from deep inelastic lepton-proton scattering and used to make absolute predictions for μ-pair, W, Z and jet cross sections in proton-antiproton collisions.

The determination of deep inelastic lepton-proton scattering in terms of deep inelastic lepton-quark scattering times the distribution of quarks in the proton is completely equivalent to the use of the short distance operator product expansion. Such a partonic description is thus as solid and well founded as any result obtained in a four-dimensional field theory.

When two hadrons initiate a hard scattering process the operator product expansion is not effective and the partonic description is the only available formalism. Here factorization is nontrivial. For example, in Z production in proton-antiproton collisions the proton interacts with the antiproton to produce many low transverse momentum pions in addition to the Z. At first glance, it would appear that such interactions are non-factorizable since they involve different interactions of the proton than occur in lepton-proton scattering. It was one of the important achievements of the 1980's to argue convincingly that hard scatterings initiated by hadron-hadron collisions factorize.

Since factorization is the foundation on which so many predictions of high energy hard interaction are based (including predictions for the production rates of top quarks, Higgs particles and various supersymmetric particles) it is important to have rigorous arguments for factorization at the leading twist level, to better understand the nature of higher power corrections and to determine to what extent they can be described in terms of partons and/or higher twist operators.

4.2 Parton Distributions

The quark distribution $q_f(x, Q^2)$ is the average number of quarks of flavor f and longitudinal momentum fraction x in the infinite momentum frame wavefunction of the proton[59]. The quarks are bare at a transverse coordinate scale $\Delta x_\perp \sim 1/Q$. The spin averaged quark and gluon distributions of the proton have been reasonably well determined over a fairly wide region of x and Q^2 from deep inelastic lepton-nucleon scattering experiments. This gives an average picture of an unpolarized proton in terms of its bare quark and gluon constituents. It would be very interesting to have a similarly detailed picture of a polarized proton in terms of quark and gluon spins.

Polarized quark distributions give much information on chiral symmetry-breaking. For example, the Bjorken sum rule gives g_A, the coupling of the axial vector current to the proton, as

$$,_1^P - ,_1^N = \frac{g_A}{6}\left[1 - \frac{\alpha}{\pi} - 3.58\left(\frac{\alpha}{\pi}\right)^2 - 20.2\left(\frac{\alpha}{\pi}\right)^3 + \cdots\right] \quad (1)$$

in the $\bar{M}S$ scheme with $\alpha = \alpha(Q)$ and where $,_1^P$ and $,_1^N$ are the first moments of the $g_1(x, Q^2)$ structure functions of the proton and neutron respectively. $g_1(x, Q^2)$ gives the number density of longitudinally polarized quarks in a longitudinally polarized proton. The difference of g_A from one is a direct consequence of chiral symmetry breaking.

An even more interesting link to chiral symmetry comes from determining the total amount of the proton's spin carried by bare quarks from polarized parton distributions. The constituent quark model predicts that most of the proton's spin should be carried by bare quarks, but with little of the spin carried by strange quarks. On the other hand, Skyrme models suggest that strange quarks carry a significant amount of the proton's spin, though the total spin carried by all flavors of quarks is predicted to be small. The experimental situation is summarized in Section 3.4. The issues here are very important for a good understanding of the wavefunction of the proton and, in particular, whether the constituent quark model can adequately describe chiral symmetry breaking or whether that symmetry breaking must be introduced more explicitly through a low energy effective theory like the Skyrme model. Our theoretical understanding of these issues has grown considerably over the past five to six years, and continued progress can be expected in the future.

4.3 α_S-Determinations

Since the early days of QCD analyses a great deal of attention has been given to determining α_S, or equivalently the Λ parameter of QCD[60]. It has become conventional to give α_S in terms of its value at the mass of the Z. At present, an average over the various ways of determining α_S from experiment gives $\alpha_S(M_z) = 0.118$ with an error between $\pm$ 0.007. It is remarkable that such diverse methods of determining α_S as event shapes in Z decay, hadronic decays of the τ and the analysis of scaling violation in deep inelastic scattering give compatible results. α_S-values obtained from some recent analyses are shown

Figure 4: Summary of the Q^2 dependence of α_S(Q). The lines indicate the QCD predictions in NNLO for four different values of $\Lambda^{(5)}_{\overline{MS}}$. (From Ref. [61]).

4.4 Higher Order Calculations

Higher order calculations are at the heart of comparing QCD theory and experiment[59]. Next-to-leading order corrections are required in order to keep factorization scale dependence down to an acceptable level and to obtain reliable normalizations. There are now a relatively large number of processes, such as the cross section for electron-positron annihilation into hadrons, the τ-lepton hadronic decay rate and the Bjorken sum rule, for which higher order corrections have been done through order ${\alpha_S}^3$. For two-jet production in hadronic collisions and for three-jet production in electron-positron annihilation the one-loop corrections have been calculated while for deep inelastic lepton scattering and the Drell-Yan process parts of next-to-next-to-leading order corrections have been done. There are now vigorous programs underway to calculate the next-to-leading order terms for four-jet production in electron-positron annihilation and for three-jet production at hadronic colliders. Recently, resummation techniques have been developed and calculations performed which allow application of QCD predictions near the edge of phase space for jet production in electron-positron annihilation and for the Drell-Yan process.

The progress made in performing and understanding higher order QCD corrections has been impressive. However, the complexity of calculation grows exceedingly rapid with the order of the higher order correction when a straightforward calculation of Feynman diagrams is performed. In the past few years an approach inspired by string theory has been developed which may effectively organize the large number of perturbative diagrams into simpler structures.

It is important to continue to develop new techniques which allow higher order calculations to be applied to more complicated processes, for example, multi-jet production, and which extend present calculations to ever higher order. It would be very interesting to have corrections at order ${\alpha_S}^4$, one order beyond what is presently available, for a number of different processes. At this order the approach of the perturbation series toward its asymptotic form should be emerging. In addition, calculations at this order are important in matching perturbative and nonperturbative contributions and for understanding scale fixing.

4.5 Jets

Because of confinement in QCD, individual quarks and gluons cannot be isolated. However, the short distance and short time part of a high-energy hard reaction is described in terms of quarks and gluons. At later times and longer distances these quarks and gluons evolve into well-collimated sets of high-energy hadrons called jets. Thus, a jet is the directly measurable quantity which comes closest to a quark or gluon. Measurement of jet cross sections are, effectively, measurements of quark and gluon scattering cross sections. Indeed, the early jet observations made at SPEAR, and a little later but more clearly at PETRA and PEP, were crucial in establishing quarks and gluons as "real" entities.

Understanding jet production and identification at a very refined level is important for many diverse reasons:

- Jets can be a background masking new physics.
- Jets may be useful in discovering new particles, such as the Higgs Particle.
- A discrepancy between theory and experiment in extremely high p_t jet production would give the earliest signal for quark substructure. Present limits from Fermilab indicate that quarks are point-like down to 1.4×10^{-17}cm.

The QCD theory of jet production and jet evolution into hadrons has developed over the last 20 years into a sophisticated and precise description of most aspects of jet physics. The early stages of jet evolution are well described by coherent QCD branching. General properties of this branching such as the momentum dependence of single particle distributions, the average multiplicity of produced hadrons and multiplicity fluctuations are known in analytic form. Detailed properties of jet evolution can be obtained from Monte Carlo implementations of coherent QCD branching. The very final stages of jet evolution, when quarks and gluons turn into hadrons, is not well understood in a fundamental way. However, there are good phenomenological descriptions of this conversion of partons to hadrons which once fixed can be used for jets at all energies independently of how the jets are produced.

Comparison between theory and experiment in jet physics has reached a level of accuracy of about 10 percent, a remarkable achievement in strong interaction physics. Major questions, however, need to be better understood. The identification of jets with quarks and gluons is clearly not perfect since jets have no color. It is important to understand the fundamental limitations to jet physics. For example, in present jet algorithms there are $1/Q$ (with Q the energy of the jet) corrections to perturbative predictions which depend on the details of the final fragmentation of quarks and gluons into hadrons. Is it possible to find algorithms which eliminate these corrections? Perhaps there are observables, unrelated to our present view of jets, which more efficiently express the physics of hard parton-parton scattering.

4.6 Exclusive Processes

Exclusive processes such as wide angle elastic hadron-hadron scattering and elastic lepton nucleon scattering do not yet furnish precise tests of QCD but they have some unique and unusual features which illustrate essential features of gauge theories[62].

It is generally agreed that perturbative QCD determines the hard part of an exclusive reaction at sufficiently high energy. There is not general agreement as to what energy is necessary for perturbation theory to apply, however. One part of the problem is knowing the exclusive wavefunctions of hadrons while another part of the problem is to better understand Sudakov effects which help an early application of perturbative QCD by forcing the valence quarks to be in a more point-like configuration than otherwise might be expected. There has recently been considerable progress in understanding Sudakov effects. There is not yet consensus, however, on the shape of exclusive wavefunctions. This is a difficult nonperturbative problem but one for which considerable progress should be possible using lattice gauge theory and light-front quantization techniques.

Whether or not short distance effects dominate exclusive processes at moderate momentum transfers can be tested experimentally. A hadron in a point-like configuration of its wavefunction should interact weakly, through its small color dipole moment, with nuclear matter. This is the phenomenon of "color transparency." By measuring quasi-elastic reactions in nuclei the effective sizes of hadrons partaking in a hard exclusive reaction can be determined. Early experiments at Brookhaven and SLAC have given intriguing but inconclusive results[63]. New results are expected soon from Brookhaven and Fermilab. These experiments and the physics issues which they shed light on lie at the interface of particle and nuclear physics. With vigorous experimental programs at Brookhaven, Fermilab, and with a somewhat upgraded energy at CEBAF, a good understanding of the space-time regions involved in hard exclusive processes should emerge in the next five to ten years.

4.7 The QCD Perturbation Series

The perturbative expansion, for measurable quantities, is certainly not a convergent expansion in QCD[64]. This is signalled by the presence of factorially growing coefficients. At present three known sources of $n!$ terms, multiplying ${\alpha_S}^{n+1}$ in the perturbation series, are known. They are ultraviolet renormalons, infrared renormalons and instanton-anti-instanton pairs. Instanton-anti-instanton pairs reflect the factorial behavior due to graph counting, while ultraviolet and infrared renormalons reflect ultraviolet and infrared renormalization logarithms in internal Feynman integrals. Ultraviolet renormalons do not hinder a reconstruction of observables from perturbation theory by using a Borel transform; however, infrared renormalons and instantons indicate that QCD perturbation theory is missing essential information.

For certain quantities like the total electron-positron annihilation cross section into hadrons, the τ-lepton hadronic width and the Bjorken sum rule the important $n!$'s, due to the leading infrared renormalons, can be removed and the missing nonperturbative information inserted using higher twist terms called QCD condensates[65]. However, the questions of scheme dependence and uniqueness have not yet been answered. Also, there are quantities like the Drell-Yan cross section where infrared renormalons are especially important but do not seem to be related to normal QCD condensates.This same phenomena occurs in heavy quark effective theories. These are far from academic problems. In many cases higher twist terms are important for an accurate description of data, and it is now apparent that the higher twist terms and high orders of perturbation theory are inextricably related.

Partly stimulated by work on possible baryon number violating effects in the electroweak theory at high energy, there has been renewed interest in instantons in intermediate energy interactions. It is clearly important to clarify whether or not knowledge of specific instanton-anti-instanton configurations provides sufficient information to remove the $n!$'s due to graph counting in QCD. There has been some early work in this direction.

Work on the nature of the QCD perturbation series and connections to higher twist terms is exciting and it can be expected that much progress will be made in the next five-ten years. Such work concerns the very nature of asymptotically free field theories. At the same time practical applications are at hand.

4.8 Small-x Physics

Small-x physics has recently become one of the most active areas of QCD research both for theorists[66] and for experimenters. This field has been greatly stimulated by recent data at HERA showing a rapid rise of the proton structure function, F_2, with decreasing x.

Perhaps the most important goal in small-x physics is to reach high enough energies (small enough x) so that parton densities in the proton become sufficiently large that the parton picture breaks down and a new strong field regime of QCD is reached. This is often referred to as the parton saturation regime of QCD. This limit of QCD has many features in common with the early stages of formation of the quark-gluon plasma which is expected in high-energy heavy ion collisions. However, in the small-x case the focus is on partons having transverse momentum in the multi GeV range while in heavy ion collisions dense partonic systems with such high transverse momentum partons are unlikely.

A second goal is to study the approach to the dense partonic regime. On theoretical grounds it has long been expected that parton distributions would exhibit the rapid growth at small values of x which has now been seen at HERA. Such a rapid growth of a cross section cannot be sustained over too large a range in $\ln(1/x)$ before unitarity corrections become important. Such corrections may be important in the energy regimes available at HERA and Fermilab. These corrections are expected to dampen the small-x growth.

In many respects the small-x problem, including unitarity corrections, resembles that of solving a two-dimensional field theory. There are now vigorous attempts in the particle physics and mathematical physics communities to reformulate small-x behavior in terms of a definite two-dimensional field theory.

Small-x behavior also has much in common with the high-energy behavior of the total cross section for hadron-hadron scattering, a process clearly dominated by nonperturbative QCD. Indeed, as Q^2 becomes small the small-x behavior of F_2 is expected to weaken and closely resemble the slow growth in energy of total hadronic cross sections. Thus, progress in small-x behavior is likely to lead to a renewed interest in trying to understand high-energy hadronic scattering at small momentum transfer, a process for which there is a highly developed, and successful, phenomenology but not yet a real connection to the fundamental degrees of freedom in QCD.

Other processes closely related to small-x behavior are diffractive scattering in deep inelastic lepton-proton interactions, recently measured at HERA, and hadronic collider events having large rapidity gaps bordered by jets, recently seen at Fermilab.

Small-x physics is still in its infancy. Its relations to heavy ion physics, mathematical physics and soft hadron physics along with a rich variety of possible experimental signatures make it central for QCD studies over the next decade.

5 QCD and Dense Matter

5.1 Introduction

Dense states of hadronic matter are believed to occur in nature in three places: in atomic nuclei, in the interior of neutron stars, and within the first millisecond of the evolution of our universe. The first of these, atomic nuclei, are generally the subject of the discipline of nuclear physics, but they are also of interest to high-energy physicists because, as we shall discuss below, there exist certain aspects of perturbative QCD that can be studied more advantageously in interactions between hadrons and nuclei than in hadron-hadron collisions. Hadronic matter in neutron stars and in the early universe can be characterized by two bulk thermodynamic quantities: the temperature T and the baryon chemical potential μ_B. In the early universe hadronic matter was essentially baryon symmetric ($\mu_B/T \approx 10^{-9}$), whereas in the inner core of neutron stars thermal effects are negligible ($T/\mu_B < 10^{-5}$).

Quite general arguments indicate that the internal structure of hadronic matter changes drastically when $\mu_B, T \gg \Lambda_{QCD}$, because the interactions between quarks and gluons become weak at high densities. The high density phase, usually called the *quark-gluon plasma*, is characterized by a lack of spontaneous chiral symmetry breaking and of local quark confinement, thus its properties are very different from those of low density hadronic matter, which is well described as a gas of weakly interacting hadrons.

The quark-gluon plasma is of more than academic interest, because conditions required for its existence can, most likely, be produced in highly energetic collisions between heavy nuclei that will be studied before the end of the present decade at the Brookhaven Relativistic Heavy

Ion Collider (RHIC), and later at even higher energy at the CERN-Large Hadron Collider (LHC). The physics of nonabelian gauge fields at high temperature, which is of central importance in the evolution of the early universe, is experimentally accessible only in the context of QCD. Methods developed theoretically and results obtained experimentally at RHIC will be seminal for other areas of particle cosmology. This aspect, together with the potential for the discovery of new forms of hadronic matter, underpins the importance of RHIC for particle physics.

Our discussion of the current status of the field, and of the immediate and long range goals will focus on three conceptually different, but interrelated issues: Hadron-nucleus interactions at high energy, QCD at finite temperature, and QCD aspects of relativistic heavy ion collisions.

5.2 QCD and Hadron-Nucleus Interactions

5.2.1 Anomalous A-dependence

Hadron-nucleus collisions have played a key role in testing QCD as a theory of the strong interaction. Although first discovered almost twenty years ago, anomalous nuclear dependence in hadron-nucleus collisions [67,68] received little attention until very recently. It is now recognized that it represents a unique physical observable that cannot only provide new tests of QCD dynamics, such as multi-parton correlations which are normally difficult to measure in hadron-hadron collisions, but also probe the nuclear structure at high energy, which is crucial for understanding and extracting quark-gluon plasma signals from relativistic heavy ion collisions.

The A-dependence in jet and single particle production is also known as the "Cronin effect". The invariant cross section for single particle production in hadron-nucleus collisions is proportional to A^{α} where α is a function of the momentum of the produced particle and can be as large as 1.3 [69,70]. Theoretically, it is agreed that multiple scattering is responsible for the observed anomalous nuclear dependence [71]. Until recently, calculations for the multiple scattering were based on addition of a number of single Born cross sections, and consequently, the results were sensitive to the infrared cutoff [72]. It was recently shown that double scattering can be consistently treated in perturbative QCD in terms of the factorization where the hard cross section is infrared safe and non-perturbative matrix elements are well-defined [73].

As already discussed in Sections 3.5 and 3.9, J/ψ suppression is considered as a possible signal for the formation of a quark-gluon plasma in relativistic heavy ion collisions. Experiments at Fermilab and CERN have revealed a strong J/ψ suppression in hadron-nucleus collisions [74,75], possibly invalidating the usefulness of J/ψ suppression as a quark-gluon plasma signal. Several models have been proposed to explain the nuclear suppression, which are based on completely different physical pictures, but seem to explain the data equally well [76,77,78]. This makes it difficult to extrapolate the observed suppression to nucleus-nucleus collisions. More work is needed before the prospects of J/ψ production as a quark-gluon plasma signature can be reliably assessed [79].

5.2.2 Multiparton Correlations

The predictive power of perturbative QCD as applied to hadrons relies on the factorization theorem which states that a physical observable can be factorized into a series of perturbative QCD cross sections and nonperturbative, but universal parton distributions. The well-known twist-2 parton distributions, which can be interpreted as the probability densities for finding a parton within a hadron, provide the leading term in this expansion. The next-to-leading term is given by the twist-4 matrix elements, which are known as four-parton correlation functions [73,80]. Knowledge of these correlation functions is crucial for understanding the non-perturbative aspects of QCD beyond the probabilistic parton distributions.

The actual size of the non-leading terms is very important for precision tests of QCD, in particular, for tests of QCD beyond the simple collisions between two partons. Because of the dominance of the leading term, it has been difficult to extract information on the non-leading terms from reactions involving isolated hadrons. It is here where nuclear targets can be of help [81].

A strong nuclear dependence in the two-jet momentum imbalance, known as acoplanarity, has been found in hadron-nucleus as well as in photon-nucleus collisions [82,83]. Since the acoplanarity due to radiation of additional partons should be the same in hadron-hadron and hadron-nucleus collisions, it is not expected to exhibit a strong nuclear dependence. The observed anomalous effect must therefore be caused by multiple scattering of final state partons while they travel through nuclear matter. This fact can be utilized not only to derive parton-parton correlations in the nuclear structure functions, but also to provide information on interaction between a colored parton with nuclear matter [84].

5.2.3 Color Transparency

In hadron-hadron elastic scattering at large angles, only small-size configurations contribute. The nucleus can act as a filter permitting only these small-size components of the incident hadron wavefunction to penetrate deep into the nucleus and scatter elastically off nucleons in the core of the nucleus [85,86]. This phenomenon, commonly known as "color transparency", was already discussed in Section 4.6. After the hard collision, the scattered hadron will initially also be in a small-size configuration which eventually expands into the full sized final state hadron. The nuclear dependence of elastic scattering can therefore provide information on the formation time of the final state hadron [87].

5.2.4 Nuclear Shadowing

At small x, the parton densities in a nucleus become so large that the sea quarks and gluons overlap spatially and the nucleus cannot be viewed as a collection of uncorrelated nucleons. This occurs when the longitudinal size of a parton, in the infinite momentum frame of the nucleon, becomes larger than the size of the nucleon. Partons from different nucleons then interact and annihilate, effectively reducing the parton density in the nucleus. This shadowing effect can be described by nonlinear corrections to the parton evolution equations that describe the parton fusion processes. Whereas a considerable amount of information about the shadowing of sea quarks exists today [88,89], the experimental and theoretical understanding of gluon shadowing is still quite limited.

Parton distribution functions at small x in very large nuclei may be systematically calculable within the framework of perturbative QCD, because there exists a new large scale parameter in the area density of valence quarks. This allows for a systematic exploration of the onset of screening of partons and the consequent shadowing of parton distributions observed in deep inelastic scattering on large nuclei [90]. This new approach could also prove to be useful as basis for a perturbative description of particle production in the central rapidity region in collisions between heavy nuclei.

5.3 QCD at Finite Temperature

5.3.1 The QCD Phase Transition

The case of baryon-symmetric hadronic matter ($T \neq 0,\ \mu_B = 0$), which is relevant to the early universe and to heavy ion collisions at collider energies, is much better understood than the general case of dense hadronic matter ($T,\ \mu_B \neq 0$), because computer simulations of lattice QCD have been feasible for this case. The numerical results (see Figure 5) show that bulk thermodynamic quantities, such as energy and entropy density, exhibit a strong structural change – probably a true phase transition – around a critical temperature $T_c \approx 150$ MeV for QCD with two light quark flavors [91]. The transition is accompanied by a rapid change in the strength of the light quark condensate, which plays the role of the chiral order parameter.

The order of this chiral phase transition is of considerable phenomenological importance. Universality arguments predict that there is a second-order transition

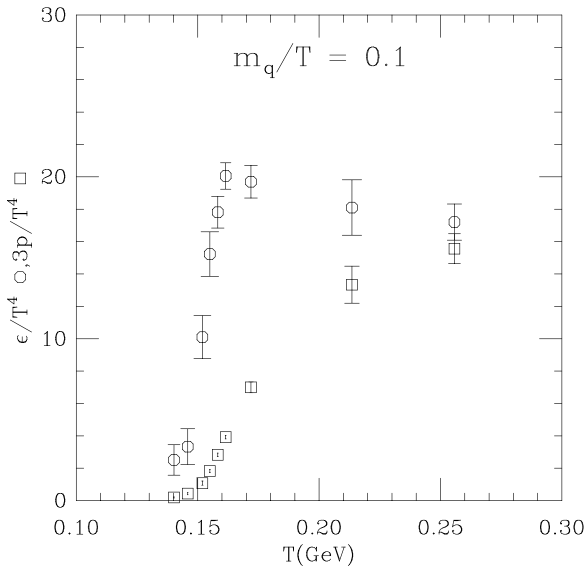

Figure 5: Energy density and pressure for two-flavor QCD on lattices with temporal extent $N_\tau = 4$. (From Ref. [91])

.

for QCD with two massless quark flavors [92,93]. As discussed in more detail in Section 6.2.3, lattice results for two very light quark flavors and one medium heavy quark flavor confirm this by not revealing hysteresis effects, at least for presently accessible lattice sizes [94,95]. On the other hand, bulk thermodynamic quantities exhibit a very rapid change in the vicinity of T_c, indicating the possibility of a weak first-order transition or of a rapid cross-over between regimes with different structure but without singular behavior of thermodynamic quantities. Simulations on much larger lattices, of order 100 lattice spacings in each of the spatial directions, are required in view of the large mismatch between the light quark masses and the QCD scale parameter Λ.

The development of numerical techniques for the study of lattice-QCD at nonvanishing baryon chemical potential remains a long term goal which, if it could be achieved, would significantly improve our understanding of the physics of neutron star cores and of relativistic nuclear collisions at energies accessible in fixed target experiments.

5.3.2 Hadrons in Medium

The structure of the low-temperature phase appears to be well described as a weakly interacting gas of mesons, in good agreement with results obtained by chiral perturbation theory and by methods based on QCD sum rules. The main potentially observable effects are shifts in hadron masses, with the general tendency to restore degeneracy of parity doublets, and changes in the width of unstable mesons. The medium modifications appear to be especially sensitive to an increase in the net baryon density. It is possible that dense cold baryon matter contains a strong component of strange hadrons, maybe in form of a kaon condensate. Thermal excitations are predicted to be less effective in inducing medium modifications of hadrons, except in the immediate vicinity of the phase transition [96].

5.3.3 Quark Gluon Plasma

Most numerical results of lattice gauge theory for the high temperature phase are in good agreement with the picture of a weakly interacting quark-gluon plasma, and are well described by thermal QCD perturbation theory, if the nonperturbative changes in the quark and gluon condensate are taken into account. The energy of an isolated quark at $T > T_c$ is finite and its color charge is screened at short distance by plasma polarization.

However, some nonperturbative features survive even at very high temperature. In particular, space-like Wilson loops continue to obey an area law, in agreement with arguments based on dimensional reduction to three-dimensional QCD [97,98,99]. As a result, space-like correlators of hadron currents remain strongly localized although color charges are deconfined [100]. This puzzling phenomenon occurs at the energy scale g^2T (g is the QCD coupling constant), where the thermal perturbative expansion diverges due to the absence of screening of static color-magnetic fields in perturbation theory [101]. However, the survival of spatial correlations appears to have a negligible effect on thermodynamic quantities and on the propagation of isolated quarks according to the lattice simulations. The phenomenological implications of the survival of space-like hadronic correlations in the high temperature phase require further study.

Several other phenomenologically relevant transport properties of the quark-gluon plasma are also known to be sensitive to the physics at the scale g^2T, in particular, various dissipation rates such as color conductivity [102], the damping rate of collective excitations [103], and the entropy growth rate [104]. A better theoretical understanding of the infrared limit of thermal gauge theories and of the physical mechanisms operating at the inverse length scale of order g^2T is needed [105].

5.4 QCD and Relativistic Heavy Ion Collisions

Relativistic heavy ion collisions afford the unique possibility to study QCD at high density in the laboratory. The basic questions are whether a quark-gluon plasma can be formed in these reactions, and if so, for what range of energy and nuclear size, and how it can be detected experimentally. The collision between two nuclei is an enormously complicated problem, since one has to deal with the evolution of a complex system of many particles from an almost pure initial quantum state into a very complicated final state best described by a statistical ensemble. This is a fundamental problem in statistical physics, here with the added difficulty that relativity is a crucial ingredient. The solution of the conceptual and technical difficulties posed by relativistic heavy ion collisions will bring many new insights and should help us better understand some basic aspects of statistical physics.

5.4.1 Thermalization

There has been a great deal of progress in the past few years in our understanding of the processes leading to the formation of a thermalized QCD plasma in a nuclear collision, and it now appears that perturbative QCD can be applied to describe the formation process [106,107], at least at high collision energies where perturbative interactions among partons, often called mini-jets, constitute an important contribution to the energy deposition mechanism. The evolution from the initial parton distributions of the colliding nuclei into a locally thermalized phase-space distribution of quarks and gluons in the central rapidity region can be visualized as a multiple parton cascade [108]. An example of the particle multiplicity distributions predicted by theoretical models (here the HIJING model [109]) based on these concepts is shown in Figure 6.

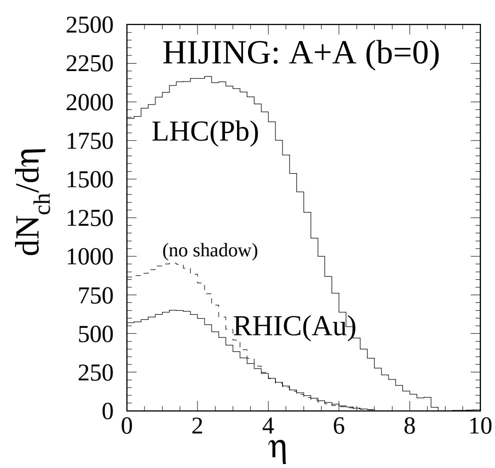

Figure 6: Predictions of the HIJING model [109] for charged particle multiplicity distributions versus pseudorapidity for central Au+Au collisions at RHIC and Pb+Pb collisions at the LHC.

The parton cascade model presently relies on two parameters that artificially cut off the infrared singularities of perturbative QCD cross sections: the minimal momentum transfer in parton-parton interactions, $p_T^{min} \approx 2$ GeV/c, and the minimal virtuality in radiative processes, $\mu_0 \approx 0.7$ GeV, which are determined from hadron-hadron collision phenomenology. These parameters may have to be modified before they can be applied to nuclear collisions. Recent theoretical studies [110,111] indicate that the infrared singularities can be regulated dynamically by medium effects in relativistic heavy ion collisions, due to color screening and collision-induced radiation suppression. If this can be implemented into the parton cascade approach, parameter independent predictions for the initial phase of high-energy nuclear collisions would be possible.

5.4.2 Quark-Gluon Plasma Signatures

As mentioned in Section 3.9.1, the experimental observation of the formation of a quark-gluon plasma relies on a variety of probes carrying information about the structure of the deconfined, chirally restored phase. Quantitative predictions for these signatures are quite sensitive to the dynamics of the thermalization and consecutive evolution of the plasma.

Numerical studies of partonic cascades have shown that the phase space distribution of gluons becomes quasi-isotropic on a timescale of 0.5 fm/c, through a combination of two-body collisions, radiative processes, and free-streaming separation of partons with different rapidities. Chemical equilibration of parton flavors takes considerably longer, of the order of 2 fm/c. The short time-scale for the thermalization of gluons implies the formation of a very hot ($T \geq 500$ MeV) initially gluon-dominated QCD plasma. This "hot glue" scenario has important phenomenological consequences: the spectra of electromagnetic signals (lepton-pairs and photons) are predicted to be much harder than previously thought, prevailing over backgrounds up to several GeV/c in transverse momentum or invariant mass, and there may be substantial thermal and epithermal contributions to charmed meson yields [112].

These signals constitute experimental probes of the earliest stages of the nuclear collision. Other proposed signatures for the formation of a quark-gluon plasma are the suppression of heavy vector mesons ($J/\psi, \psi', \Upsilon$), the enhanced production of strange hadrons (especially strange antibaryons), and kinematic consequences of the existence of a mixed phase. A comprehensive assessment of these signatures in nuclear collisions is needed, in order to find the best combination of signals that can establish the formation of a locally color-deconfined phase with restored chiral symmetry [113].

5.4.3 Hadronization and chiral transition

As the quark-gluon plasma expands and cools, it eventually reaches the hadronization threshold. Present wisdom is that the hadronization (chiral) phase transition is of second order and hence allows for long range fluctuations of the chiral order parameter. Numerical studies have recently shown that, if this transition proceeds out of thermal equilibrium, fluctuations in temporarily unstable infrared modes can develop into extended domains characterized by a misaligned chiral order parameter [114,115,116]. Such a "disorientated chiral condensate" would eventually decay into a collective low-energy excitation of the pion field resembling an isospin singlet pion laser. This scenario would have dramatic experimental signatures, most notably a highly unusual charge ratio of the emitted pions, with a large probability for the strong depletion of neutral pions (see Section 3.9.1).

The dynamics of the chiral phase transition out of equilibrium is still poorly understood. Considerable progress has been recently made through a combination of lattice simulations and modelling of instanton effects on the origin of chiral symmetry breaking in QCD [117]. More work is required to extend these studies to dynamical properties of the quark condensate in the vicinity of the phase transition.

5.4.4 Strange quark matter

The baryon-rich quark gluon plasma, which may be formed in nuclear collisions at presently accessible energies, is characterized by a high content of strange quarks. The strange quark concentration can be further increased by distillation mechanisms during hadronization, opening exciting prospects for the formation of multiple hypernuclei and, quite possibly, of multi-strange quark matter droplets that might have a long life-time. Experimental searches for such new metastable states of nuclear matter ("strangelets") are under way [118,119,120]. Improved models for the description of hadronic matter with a high strangeness content, possibly based on ideas of chiral perturbation theory, need to be developed.

5.4.5 Nonperturbative effects

Semiclassical studies indicate that there exist efficient nonperturbative mechanisms that transfer energy from high-energy to low-energy modes in gauge theories. A better understanding of the meaning of (semi-) classical solutions in the framework of quantum field theory could shed light on this issue, which has potential implications, besides QCD, for nonperturbative electroweak processes, such as multiparticle production at ultrahigh energies and baryogenesis. A long term goal is to find a practicable scheme for the study of nonequilibrium processes in the framework of lattice QCD. This would also facilitate investigations of the nonequilibrium aspects of the hadronization process, which hold considerable promise of providing unambiguous signatures for the occurrence of a phase transition in relativistic heavy ion collisions.

5.5.1 Chiral perturbation theory

Low energy effective theories of QCD are a powerful tool in strong interaction physics. They have been successfully applied to electroweak decays of hadrons [121,122], to low energy hadron scattering [123,124], and most recently, to few nucleon systems [125,126,127]. Many of these theories make use of the approximate chiral invariance of the QCD Lagrangian caused by the near masslessness of the light quark flavors u, d, and to a lesser extent, s. The gradient expansion of the chiral field allows for a systematic perturbation theory approach, at energies much lower than the chiral symmetry breaking scale $\Lambda_\chi \approx 1$ GeV, which conserves all symmetries of full QCD.

There are a number of interesting new results in QCD at low energy. The properties of the pseudoscalar mesons (π, K, η) have been studied in great detail using chiral perturbation theory to two loop order. There are a large number of free parameters which must be fit, but there are a far greater number of experimental measurements which can be predicted. The results are in excellent agreement with the experimental data. Previous discrepancies, such as in $\gamma\gamma \to \pi^0\pi^0$ have all been resolved using the new two-loop results [128].

Chiral perturbation theory has also been successfully applied to the baryon sector. It was thought that chiral corrections to the baryons were large, and that chiral perturbation theory might not be that useful for the baryons. However, it has been shown how one can consistently apply chiral perturbation theory to the baryons, with small corrections [129]. The basic idea is that one must include both the nucleon and the Δ resonance in the chiral Lagrangian, since there is a large $\Delta N\pi$ coupling. The loop effects of intermediate $\Delta's$ and nucleons cancel, so that the radiative corrections are under control. The baryon calculations are still in their infancy, compared with the sophisticated results obtained for the meson sector.

5.5.2 Large N_c expansion

The $1/N_c$ expansion (N_c is the number of colors) provides a means of computing hadronic quantities in a systematic expansion in QCD [130,131]. In the mesonic sector, the $1/N_c$ expansion can be used to obtain relations between chiral Lagrangian parameters that are well satisfied experimentally [132]. The $1/N_c$ expansion has also been used to justify certain features of QCD inspired models of hadrons, such as the Nambu-Jona-Lasinio model. Recently, the $1/N_c$ expansion has been used to obtain systematic predictions for baryons in QCD [133]. Some results, which are proved up to order $1/N_c^2$, are in excellent agreement (15%) with experiment.

5.5.3 Applications

QCD is known to provide an excellent description of strong interaction dynamics. The computations of low energy hadron properties at the 10% level are not accurate enough to provide a precision test of QCD. Nevertheless, these calculations are very important, and should be pursued in the future. Firstly, tests of the electroweak theory invariably require knowledge of hadronic matrix elements, and these can be calculated using the methods discussed above. For example, the prediction of rare K decay rates or ϵ'/ϵ in the standard model requires knowing the matrix elements of 4-quark operators between K and π states. The sensitivity to deviations from the standard model is limited by how accurately one can calculate these hadronic matrix elements. Secondly, QCD provides us with a testing ground for the theoretical methods used to study non-perturbative effects in gauge theories. Non-perturbative effects may well be responsible for electroweak symmetry breaking (either through technicolor, or by dynamical supersymmetry breaking). It is important to test the theoretical ideas on QCD to see how well they work, before applying them to new theories.

6 Lattice QCD

6.1 Introduction

Many important features of QCD lie outside the reach of perturbation theory. In order to study them one must resort to non-perturbative techniques. In particular, one must be able to regularize and renormalize the theory in a non-perturbative manner. The formulation of QCD on a lattice in Euclidean space-time, introduced by Wilson in 1974, provides such a regularization and establishes a powerful framework for studying the non-perturbative properties of QCD and other quantum field theories. Since its introduction, lattice QCD has formed the basis for a very large number of investigations of hadron properties. Of special importance has been the fact that the lattice regularization permits the application of numerical simulation techniques to the analysis of the quantum fluctuations. These have been used successfully to derive several quantitative predictions from the first principles of QCD[134].

Lattice QCD does not hold the unique key to the study of the non-perturbative properties of hadrons, even if we add the challenging constraint of a meaningful regularization of the ultraviolet divergences. For instance, a calculation based on the expansion into quantum fluctuations around a semiclassical solution of $O(1/g)$, even if the expansion takes a perturbative form, would embody non-perturbative effects. However, because of the very special role that the lattice formulation has played in the study of non-perturbative QCD phenomena and because of the many results that have been obtained through its application, this entire section will be dedicated to it.

6.2 Lattice QCD in Euclidean Space-Time

6.2.1 Methodology

The most important aspect of lattice QCD is that it provides a gauge regularization of the ultraviolet divergences which does not require a gauge fixing. This is accomplished by taking finite elements of the gauge group, rather than the gauge potentials $A^i_\mu(x)$ which are elements of the gauge algebra, as dynamical variables. These finite elements of the gauge group $U^{c,c'}_\mu(x)$ are color $SU(3)$ matrices and are defined over the oriented links of a lattice in Euclidean space-time[135]. In most applications this is a hypercubical lattice with lattice spacing a. Matter fields (the quark fields ψ, $\bar\psi$ in QCD) are defined over the sites of the lattice. The gauge field variables $U_\mu(x)$ and the quark fields are combined into gauge invariant expressions, which form the building blocks of the discretized space-time action. This consists of a pure gauge term $S_g(U)$, which reduces to $\int \frac{1}{4} F_{\mu\nu} F^{\mu\nu} d^4x$ in the continuum limit, and of a matter field term $S_q(\psi, \bar\psi, U)$, which discretizes the Dirac term of the continuum action. In terms of these variables the quantum expectation value of any observable is given by

$$\langle O \rangle = Z^{-1} \int dU\, d\bar\psi\, d\psi\, O(U, \bar\psi, \psi)\, e^{-S_g - S_q} \qquad (2)$$

with

$$Z = \int dU\, d\bar\psi\, d\psi\, e^{-S_g - S_q} \qquad (3)$$

If one considers a system of finite space-time volume V at first, letting $V \to \infty$ at the end of the calculations, the integrals in the two equations above are integrals over a finite, albeit very large, number of variables. These integrals are either over a compact domain (for the group elements U) or over Grassman variables ($\bar\psi$, ψ), and thus they represent mathematically well-defined, finite quantities. Since O can be any observable, Eqs. (2) and (3) provide in principle the description of all QCD phenomena. Of course, in principle is the keyword. Although the integrals are well defined, they are quite complex and calculating them, even in an approximate manner, is a formidable task. Moreover, at the end of the calculation the regulator given by the finite lattice spacing a must be removed in order to obtain continuum results. This is done by readjusting the coupling constant g which appears in S_g and determines the strength of quantum fluctuations of the gauge field. g plays the role of a bare coupling constant. In the process of renormalization g and a are sent simultaneously to zero, with a functional relation $a = a(g)$ determined in its leading orders by asymptotic freedom, in such a way that all physical observables tend to a finite limit[136].

The regularization of QCD given by Eqs. (2) and (3) is non-perturbative and permits the implementation of many calculational techniques, frequently similar to techniques used in statistical mechanics, which are not available in the more conventional perturbative schemes of renormalization. Of particular importance is the possibility of applying powerful computational methods to an approximate calculation of the quantum expectation values.

The computational analysis of lattice QCD proceeds first through the integration over the quark fields $\bar\psi, \psi$, which can be done explicitly because the matter part of the action S_q is bilinear in the quark fields. This leads to integrals over the gauge variables only

$$\langle O \rangle = Z^{-1} \int dU\, \langle O \rangle_U\, e^{-S_{eff}} \qquad (4)$$

where $\langle O \rangle_U$ stands for the average of O over the quark field fluctuations alone, in the background provided by the gauge field U, and

$$S_{eff} = S_g - \log\det[D(U)] \qquad (5)$$

$D(U)$ being the lattice Dirac operator that appears in S_q.

Because of γ_5 invariance, $\det[D(U)]$ is a positive, semidefinite quantity. $e^{-S_{eff}}$ can therefore be taken as a measure factor in the space of the gauge variables $U_\mu(x)$ and the integrals giving $\langle O \rangle$ can be approximately calculated by numerical simulation techniques. This is the essence of the computational methods underlying the majority of the numerical studies of QCD performed in the past, or envisioned for the future. There are, however, some important remarks which must be appended even to the most concise description of the methodology of lattice QCD.

• Numerical simulations techniques proceed by averaging over a very large number of "configurations" of the system (in our case the collection of all $U_\mu(x)$) distributed according to the desired measure. These are obtained through repeated "upgrades" of the dynamical variables $U_\mu(x)$, in which these are either individually or collectively replaced by new values, according to some definite stochastic or deterministic algorithm. Since the number of dynamical variables is huge and the number of upgrades required for reasonably accurate averages can also be very large, it is crucial that the upgrades be done by the computer as rapidly as possible. With a measure factor that involves only couplings between neighboring variables, such as the exponential of the pure gauge part of the action e^{-S_g}, an individual upgrade requires a small number of arithmetic operations (these can range in the thousands, but this is still a small number with respect to the typical number of dynamical variables and to the overall scale of the computation) and, in any case, independent of the volume of the system. But this is no longer the case when the non-local $\det[D(U)]$ is incorporated in the measure. Algorithms to account for the effects of the fermionic determinant, either in an approximate manner or exactly, have been introduced and are routinely applied. They require a few orders of magnitude ($10^2 - 10^4$) more arithmetic operations than are needed with a local measure alone. All of this has prompted the use of an approximation, called the quenched or valence approximation, whereby the gauge field configurations are generated according to the pure gauge measure factor e^{-S_g}. Since in field theoretic terms the fermionic determinant accounts for the creation and annihilation of virtual quark-antiquark pairs, the quenched approximation consists in neglecting $q - \bar{q}$ vacuum polarization effects. Various arguments can be given to support the validity of such approximation. Also, there is a considerable effort in lattice QCD investigations to go beyond the quenched approximation. It is a fact, however, that many computational analyses of QCD, especially those aiming at the largest lattices or smallest quark masses, have been or are currently based on the quenched approximation.

• There are some notorious problems in the lattice discretization of the continuum Dirac operator. It is not possible to define a lattice Dirac operator with the formal chiral properties of the continuum one[137]. There are formulations of the lattice Dirac operator which permit meaningful simulations of QCD, but one pays with either an explicit breaking of chiral symmetry (Wilson formulation)[135], which must be recovered through the careful tuning of a mass counterterm, or with a breaking of flavor symmetry, which is restored only in the continuum limit, and limitations on the possible number of flavors (Kogut-Susskind or staggered formulation)[138,139].

• The γ_5 invariance which guarantees the reality of $\log\det[D(U)]$ and makes it possible to incorporate the fermionic determinant in the measure is no longer true in presence of a quark chemical potential. Thus numerical studies of QCD at finite baryon number density, while not impossible, are computationally much more demanding and the results much more approximate.

• Perturbative techniques can also be applied to the lattice formulation of QCD. The perturbation expansion is more complicated on the lattice than in the continuum because of the loss of Lorentz invariance, but can still be carried out. Lattice perturbative calculations are important and have been done to determine crucial renormalization parameters and to establish a bridge to the more conventional perturbative results[140,141].

6.2.2 Hadron spectroscopy

Among the non-perturbative observables of QCD hadron masses occupy a very prominent role. Accordingly, through the years many lattice calculations have been devoted to the calculation of the hadron spectrum. One considers an observable $O(t)$ with non-vanishing matrix elements between the vacuum and the states with the quantum numbers of the hadron whose mass is being sought. O can therefore act as source for creation of the hadron, $\bar{O}$ as a sink for its annihilation. Typically O will consist of a quark-antiquark bilinear for the calculation of meson masses, a product of three quark fields for baryon masses or some expression involving the gauge fields for the study of glueballs. Also, it is convenient to project over states of zero spatial momentum by including into the definition of O a sum over spatial sites (a projection over definite, non-zero spatial momentum can also be easily implemented). One uses then simulation techniques to evaluate the Euclidean correlation function (or Green function) $\langle \bar{O}(t) O(t') \rangle$. On general grounds this is given by

$$\langle \bar{O}(t) O(t') \rangle = \sum |\langle \phi | O | 0 \rangle|^2 e^{-E(\phi)|t-t'|} \qquad (6)$$

where the sum ranges over all physical states with the quantum numbers of O and the exponential fall-off is due to the fact that one is considering Green functions in Euclidean space-time. From a numerical determination of the leading exponential behavior(s) one can then derive the energy (mass, if one has performed a projection over zero space momentum) of the lowest state(s).

The basis for such calculations was established in the early eighties[142,143]. The intervening years have brought, however, very important refinements in the construction of the source (sink) operators O ($\bar{O}$), by which crucial enhancements of the matrix elements between the vacuum and the desired hadron states have been obtained, as well as constant improvements in the scope and accuracy of the calculations[144]. The actual precision is limited by the statistical nature of the calculations as well as by a variety of systematic errors. The latter are due to the finite volume of the lattice, the finite lattice spacing, practical limitations on the quark mass (the rate of convergence of the algorithms for calculating quark propagators becomes prohibitively slow for small quark masses) and to the finite extent in Euclidean time over which one can calculate the Green function with sufficient accuracy (this limits the precision in the calculation of the masses due to mixing with higher states). In regard to this last point, it is to be noticed that the calculation of Green functions for operators built out of quark fields proceeds through an initial calculation of the quark propagators, which are then combined as appropriate and averaged over several gauge field configurations. Of the overall fall off of the Green functions, a large fraction is then due to the fall off of the quark propagators themselves, and only part to the averaging procedure. This is to be contrasted to the case of the Green functions for gluonic operators, where the entire fall off comes from cancellations among quantities which are typically of order one. As a consequence, the masses of states whose Green functions are given by connected quark lines can be determined with better accuracy than the masses of purely gluonic states (glueballs). Even worse is the situations for states that would involve disconnected quark lines, such as admixtures of q-$\bar{q}$ states and glueballs, for which up to now it has been possible to do very little with lattice techniques.

Currently, large scale calculations of the hadron spectrum in the quenched approximation involve lattices with a spatial extent ranging up to 32^3 sites, time extent up to 64 sites, ultraviolet cutoffs ranging up to $a^{-1} \approx 3GeV$ and spatial volumes ranging up to $(3-4\,\mathrm{f})^3$ [144]. The lowest values of the quark mass is best characterized by the corresponding value of the pseudoscalar mass, as it emerges from the calculation. One obtains ratios m_π/m_ρ down to ≈ 0.3 as opposed to the experimental value 0.175. Because of the current algebra relation $m_{ps}^2 \sim m_q$ the square of the pseudoscalar mass is a better indicator of the quark mass and this gives a current value $(m_{ps}/m_{vect})^2 = 0.09$ versus a target 0.03. A lot of attention is being paid to the effects of the finite lattice spacing, finite volume and other sources of systematic effects. Extrapolations based on analyses done for several values of these parameters are used to reach the physical domain. One recent study[145], based on a very careful set of extrapolations over volume, lattice spacing and quark mass, has produced a set of results in excellent agreement with the experimental data (*e.g.*, $m_N/m_\rho = 1.216(104)$ (experimental value 1.222); $m_\Delta/m_\rho = 1.565(122)$ (exp. 1.604); $m_\phi/m_\rho = 1.333(32)$ (exp. 1.327); $f_\pi/m_\rho = 0.106(14)$ (exp. 0.121). In this study m_π, m_K are used to determine the bare quark masses, while m_ρ sets the scale for the lattice spacing. The same study found a value $1740 \pm 71MeV$ for the 0^{++} glueball mass. A slightly lower but not inconsistent value of $1625 \pm 92MeV$ has recently been found by another group[146]. These values pertain to the pure gauge system and do not account for possible mixing with $q\ \bar{q}$ states which, as mentioned above, are much harder to calculate. Figures 7 and 8 illustrate the results obtained for hadron masses and for the scalar glueball decay constant in the study mentioned above[145,147].

There are also many investigations which do not rely on the quenched approximation (full QCD simulations or simulations with dynamical quarks). Since including $\det[D(U)]$ (and thus the effects of virtual q-$\bar{q}$ pairs) in the measure is algorithmically very costly, such calculations are typically limited to lattice sizes about one half of the corresponding quenched calculations. Even more important is the fact that the simulation algorithms can be effectively implemented only with rather large quark masses leading to $(m_{ps}/m_{vect})^2 \gtrsim 0.25$, versus 0.09 for the quenched approximation and the experimental value of 0.03 for light quarks. With such large quark masses

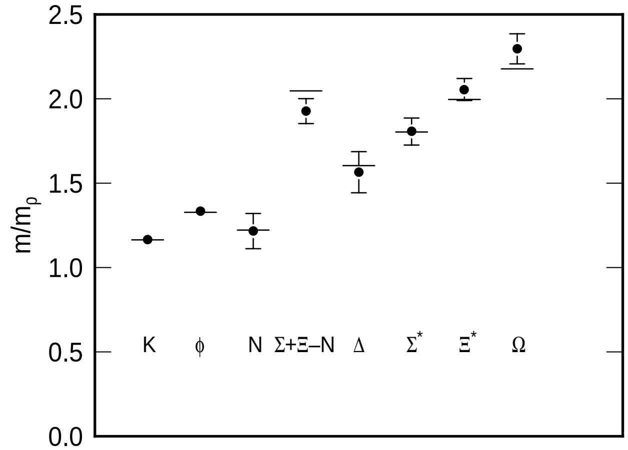

Figure 7: Masses of several hadronic states in units of m_ρ as obtained in a recent large scale quenched calculation. The horizontal lines represent the experimental values.

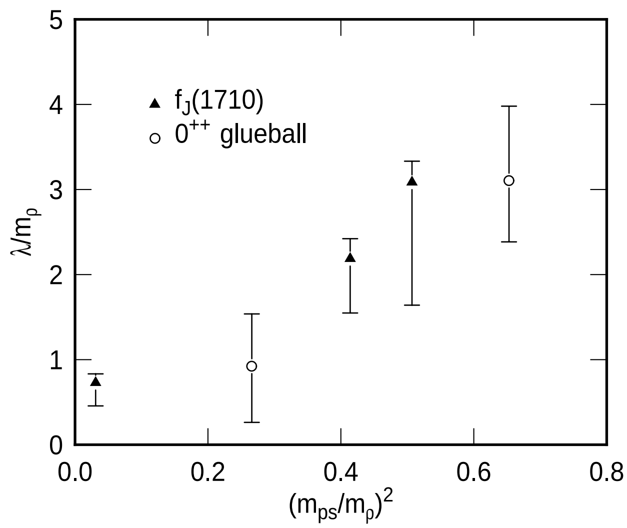

Figure 8: Decay constants of the f_0 (1720) in comparison to lattice results for the scalar glueball.

the whole effect of the fermionic determinant appears to be limited to the renormalization of the bare coupling constant and, moreover, the ratio between the masses of the nucleon and the vector meson stays very close to the heavy quark limit of 3/2. This situation is reminiscent of the earlier quenched calculations, where because of the more modest computer resources and in absence of the recent algorithmic improvements, one was similarly limited to large quark masses. It is very likely that in the near future the progress in non-quenched calculations will parallel the advances achieved by quenched spectrum calculations during the last few years.

Another set of spectral data of great interest in QCD are the masses of states containing heavy quarks. These are too large for a direct lattice calculation based on the formalism outlined above, but can still be calculated with good accuracy either by using the lattice to evaluate the potential binding the heavy quarks (and the spin dependent potentials) or by developing an effective theory to describe the degrees of freedom of the heavy quarks in a non-relativistic approximation. These approaches give origin to interesting issues of renormalization, where substantial progress has recently been made[148]. The splittings among different states in the heavy quark families can be calculated with precision, and these results can in turn be used to determine the value of the coupling constant α_S. Recently values for $\alpha^{(5)}_{\overline{MS}}$ at M_Z clustering around 0.110, with errors ± 0.008, have thus been found, with the major element of uncertainty coming from the corrections one has to make to the quenched approximation to include short-distance quark polarization effects[149]. It is to be noticed that these calculations of the strong coupling constant are already competitive with those based on perturbative QCD and that the lattice may soon provide the way to produce the most precise determinations of α_S. A compilation of values of α_S, obtained by perturbative and by lattice methods, is presented in Figure 9 [149].

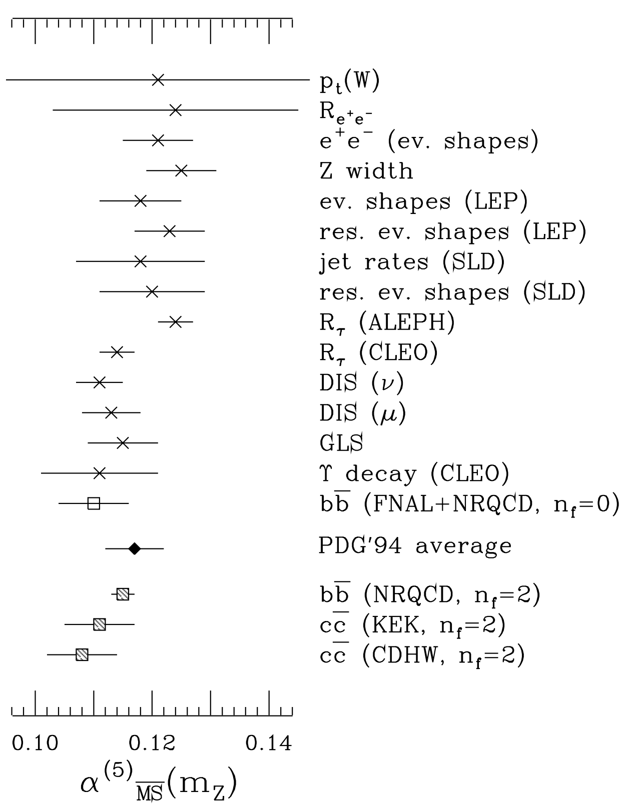

Figure 9: Compilation of results for α_S. The crosses denote results based on perturbative QCD, the boxes results based on lattice QCD. The shaded boxes represent very recent results which are not part of the PDG 1994 average.

6.2.3 High temperature QCD

The demonstration that quenched QCD undergoes a deconfining transition at a temperature of approximately $200 MeV$ was one of major successes of lattice QCD. The study of QCD at a finite temperature T proceeds through a path integral formulation of the thermal average

$$\langle O \rangle_T = Tr(Oe^{-H/T}) \tag{7}$$

The exponential is interpreted as a propagation factor for an Euclidean time $t = 1/T$ and one is thus lead to consider a system quantized in an Euclidean domain of infinite extent in the spatial directions but finite extent $1/T$ in the temporal direction, where periodic (antiperiodic) boundary conditions are imposed on bosonic (fermionic) fields to implement the trace in Eq. (7). In practice this system is simulated on a lattice of N_s sites in the space directions and $N_t \ll N_s$ sites in the time direction. The temperature is related to lattice spacing and temporal extent by $T = 1/(N_t a)$.

The properties of the deconfining transition in quenched QCD have been by now rather well established[150]. The critical temperature, the order of the transition (weakly first order) and other observables, such as the surface tension of nucleating hadrons, have been determined. Many of the current efforts are being devoted to simulating hot QCD with dynamical quarks[151,152,153]. As one would expect, the creation and annihilation of virtual q-$\bar{q}$ pairs has strong effects on the dynamics of the thermal fluctuations. These are felt even for moderately large quark masses and lattice simulations have shown that they can alter the nature of the transition. For large quark masses, of course, one expects little departure from the results of quenched QCD. For intermediate quark masses, full QCD simulations indicate a weakening of the transition, which appears to change to a rapid cross over from the hadronic medium to a quark-gluon plasma with no discontinuities. Also, the temperature of the transition is lowered with respect to the quenched case. At exactly zero quark mass there are theoretical arguments for a transition driven by the restoration of chiral symmetry, which is of the second order for two quark flavors and of the first order with $N_f > 2$. The interesting case is, of course, the one of light, but not vanishing quark masses and current investigations have been focusing on this situation. There is good numerical evidence that a first order transition persists into the domain of finite (non-zero) quark mass with four flavors of light quarks. For the more realistic case of two light quarks and one quark of intermediate mass the results are still inconclusive, but it is realistic to expect that substantial progress will soon be made.

6.2.4 Weak matrix elements

Hadronic matrix elements of weak operators are very important for extracting the parameters of the electroweak theory from the experimental data and, more generally, for testing the predictions of any fundamental theory of weak interactions against experiment. Lattice techniques can be used to calculate many of these matrix elements[154,155,156].

The difficulty in calculating these observables, and consequently the precision which can be achieved, depends a lot on the type of matrix element under consideration. If we recall that individual hadronic states are isolated on the lattice by the "filtering ability" of the propagation in Euclidean time, which enhances the contribution from the lightest states, it will be clear that matrix elements between the vacuum and a single particle state, such as those encountered in the calculation of pseudoscalar decay constants, are much easier to calculate that those involving two or three external particle states. Additional difficulties lattice calculations have to contend with, beyond the general need of correcting for finite lattice spacing, finite volume etc., come from the fact that the weak interactions frequently involve scales much larger than the lattice momentum cutoff. This can be taken care of by an operator product expansion of the interaction followed by renormalization down to the scale of lattice momenta. Problems of renormalization thus play a very important role in the lattice determination of weak matrix elements and much progress has been made in this field. Perturbative and non-perturbative methods of renormalization have been developed and are routinely used to relate the quantities calculated on the lattice with their continuum counterparts[154,155,156].

Pseudoscalar decay constants for the light mesons (f_π, f_K) are calculated together with the masses in the hadronic spectrum and the results are in good agreement with experiment. Recently much attention has been paid to the calculation of the decay constants for heavy-light mesons, f_B and f_D. Since the mass of the B meson is larger that the lattice cutoffs which can be reached in present calculations, the determination of f_B can proceed either through the use of a static approximation for the heavy meson or via an extrapolation of results obtained for lighter mesons. Earlier calculations showed a marked discrepancy between the results obtained by the two methods, but a better understanding of the static approximation and of various renormalization factors has brought the two sets of results in much better agreement. The values found for f_B thus tend to cluster around $200MeV$, with quoted errors of the order of $10 - 15\%$ and variances between the results obtained by different groups of about as much. Values $f_D \approx 210MeV$ and ratios $f_{Bs}/f_B \approx 1.1$, $f_{Ds}/f_D \approx 1.1$ are also found[155].

Quantitatively meaningful results have begun to appear for semileptonic form factors in the decays $D \to K$, $D \to K^*$, $B \to K^*\gamma$ and for the Isgur-Wise function. Another quantity for which very substantial progress has been made is B_K, the $K^0 - \bar{K}^0$ mixing parameter. It is possible to quote today a lattice value $B_K(2GeV) = 0.616 \pm 0.020 \pm 0.017$ ($\hat{B}_K = 0.825 \pm 0.027 \pm 0.023$)[157].

Many other matrix elements have been considered in the literature, including those governing the non-leptonic decays $K \to \pi\pi$, trying in particular to find a computational explanation for the $\Delta I = 1/2$ rule. As implied above, these are very challenging and for the moment cannot be calculated with confidence, but with the expected improvements in algorithms and computational resources they should also become calculable within the next few years.

6.2.5 Hadron structure and other observables

There are many more QCD observables which can be calculated by lattice techniques. Reasons of space prevent us to go at any depth into their list. Many of these observables are discussed in detail in [134]. First steps have been taken toward the calculation of structure functions. Charge density correlations within hadrons have been determined. A very interesting recent calculation has shown that these are left almost unchanged if one uses so-called cooling techniques in the simulation to suppress short range quantum fluctuations, leaving only long range instanton excitations. This points to an intriguing role played by topologically non-trivial structures in the dynamics of hadrons.

The properties of the QCD vacuum have been the subject of many investigations. Lattice techniques have been used to evaluate observables such as the magnitude of the fluctuations of the topological charge and the gluon condensate. They have helped clarify the effects of monopoles in the maximally Abelian gauge and investigate the gauge fixing ambiguities encountered for large fields. Altogether, the lattice formulation of QCD is much more than a tool for the numerical determination of experimental observables. Suitably used, it can provide valuable insights into the whole dynamics of strong interactions.

6.2.6 Discussion of the errors

Since lattice QCD calculations are based on sampling techniques, the results are affected by statistical errors. In general it is rather straightforward to estimate the magnitude of the statistical errors (exceptions are the cases where metastabilities make it difficult to reach statistical equilibrium) and these are universally quoted together with the results. Somehow more difficult is the estimate of the systematic errors coming from finite lattice spacing, finite volume, the quenched approximation (if used) and all other approximations required to implement the numerical simulations. A lot of attention is generally paid to these sources of error and various procedures, such as repeating the calculations with different lattice sizes and different values of the bare coupling constant (which, through the renormalization relation $a = a(g)$ implies different lattice spacings), are used to estimate the magnitude of the systematic effects and, if possible, to correct for them.

Nevertheless, although these (statistical and systematic) errors can be quantified, there are other elements of uncertainty which depend to a large extent on the questions which are being asked and on what one is willing to assume. This is what makes the often heard question "when will lattice calculation produce a result accurate to (say) 5% for the ratio m_ρ/m_N?" difficult to answer. Depending on what theoretical assumptions one is willing to accept, such a rate of precision has already been achieved or may be still several years far away. The recent calculation of the spectrum considered above is a case in point. Large samples of configurations have been used to reduce the statistical errors and very careful extrapolations in lattice volume and lattice spacing have been made. Still the calculation could only be performed for quark masses larger or equal to approximately one half the strange quark mass and in the quenched approximation. Recent theoretical studies, based on chiral perturbation theory, of the quenched approximation indicate that the limit of zero quark mass is singular. Taken per se this would seem to invalidate completely the extrapolation in quark mass that was used to derive the masses of hadrons made of u and d quarks: on theoretical grounds one would not trust a linear extrapolation for the quenched approximation. At the very least, one would want to see the values it produces with much lighter quark masses. But then the effects of $q - \bar{q}$ vacuum polarization effects are expected to become important and one would not trust the quenched approximation anyway. This road leads to the conclusion that the only reliable results would be those of full QCD simulations done with light dynamical quarks. Such simulations are certainly several years away.

But one can look at things from a different perspective. One can give theoretical arguments in support of the fact that hadron masses should exhibit a smooth behavior as function of the masses of the quarks. From this point of view, one can then assume the legitimacy of a linear extrapolation in m_q (using squared masses, on current algebra arguments, for the lightest pseudoscalars), which finds confirmation in the experimental data. Notice that even with this assumption, the slopes and intercepts of the linear fits remain as important, and quite non-trivial, non-perturbative observables of QCD. The lattice calculation of the spectrum, done within a range of values for m_q where the quenched approximation is expected to be valid, provides then a quantitative determination of these observables. This is a major accomplishment, for which one would have held little hope prior to the advent of lattice QCD.

6.3 Alternative Discretization Techniques

6.3.1 Null-plane quantization

The null-plane quantization is a well established, alternative method of defining a quantum field theory where one of the light cone coordinates, *e.g.*, $x^+ = (x^0 + x^3)/\sqrt{2}$, replaces the time coordinate x^0 as the evolution variable. It offers some important advantages over the more conventional $x^0 = const$ quantization, such as better properties of the vacuum state, explicit invariance under Lorentz boosts in the x^3 direction and a more direct relationship between deep inelastic structure functions and the wave-functions of quarks within hadrons. Computational techniques based on the null plane quantization have been introduced and studied during the past few years[158]. In this approach one focuses directly on the wave-functions of the hadronic components. In the restricted two dimensional space spanned by the $x^+, x^- = (x^0 - x^3)/\sqrt{2}$ coordinates the gauge field interaction produces a linear potential, which gives origin to confinement. The extension to four dimension can be accomplished by discretizing the space of transverse coordinates x^1, x^2. The challenge is then to show that confinement survives this extension of the degrees of freedom and to incorporate all appropriate renormalization effects. As a computational technique, the null-plane quantization of QCD has not been as widely studied as the Euclidean lattice formulation, but it constitutes a quite different approach with the potential of producing valuable complementary results.

6.3.2 Hamiltonian QCD and other approaches

In the Hamiltonian approach to lattice QCD one discretizes the space coordinates, but maintains a continuous time variable. The gauge dynamical variables are finite group elements associated with the oriented links of the spatial lattice (very much like in the Euclidean formulation) and their conjugate momenta, which are the components of the chromoelectric field. The evolution is in real time and is generated by a well-defined Hamiltonian operator[138]. Indeed, if one considers a system of finite volume, this is a many-body Hamiltonian with a finite number of degrees of freedom. One tries then to find good approximations for the wave function of the vacuum and of the hadrons, and for the energy levels of these states, typically by using variational techniques. The major difficulty in this approach is the need of incorporating a very large number of components in the wave functions, a problem which is bypassed in Euclidean lattice QCD by simulating directly the quantum fluctuations. Thus, unless one succeeds in producing extremely good *Ansätze* for the wave functions, there are serious limitations to the accuracy which can be achieved.

Several other computational techniques, for example methods based on the derivation of equations relating the expectation values of transport factors (Wilson loops), have been proposed and studied. In addition, one should mention the large body of analytical work that has been and is been done in the context of lattice QCD. Research in this field is indeed far from being exhausted by the numerical simulations. Perturbative calculations, done by analytic expansion techniques, play a crucial role in defining various renormalizations that must be made to bridge the gap to the continuum. Analytic methods have been used to study finite size effects, to study gauge fixing ambiguities and their implications, to calculate the spectrum of QCD in a small box, to perform large N_c and strong coupling expansions etc. Very much like what is happening in other fields of physics, in lattice QCD one is also finding that analytical and computational methods complement each other and together provide a very powerful tool for deriving quantitative predictions.

6.4 Expected Progress

6.4.1 Computational resources

Lattice QCD calculations are very demanding computer applications. The size of the lattices one can consider, as well as other important parameters such as the values of the quark mass, depend in a crucial manner on the number of variables one can store and on total number of arithmetic operations one can perform. For a computation of a reasonably limited duration, the latter converts in number of floating point operations per second (flops). Indeed, scope and accuracy of lattice QCD calculations have steadily increased over the years as computers have gained in memory capacity and speed. The pace of progress in computer technology is forecast to continue for years to come and thus one can correspondingly foresee very substantial, hardware driven improvements in lattice QCD calculations.

While the advance in computer technology is obviously quite independent of lattice QCD applications, which can thus ride the wave of commercial development, the very special computational features of such applications has stimulated the design and construction of dedicated computers, to be used exclusively (or mostly) as a laboratory for the numerical simulation of QCD[159]. The rationale behind such developments is that the highly organized structure of data and communications in QCD applications permits an optimal utilization of parallelism, so that one can gain in economy and efficiency by designing and building a supercomputer targeted to these calculations. Dedicated machines capable of sustained speeds of several Gigaflops have been built and used successfully in the US and abroad[159].

At present there are two projects within the US for dedicated QCD supercomputers capable of reaching into the Teraflops domain:

• A project pursued by a group at the Columbia University in collaboration with researchers from several other institutions plans to use digital signal processors and a rather streamlined communications architecture to achieve a peak speed of 0.8 Teraflops and a sustained speed of 0.5 Teraflops[160]. The total cost of this project is estimated at $3M.

• The QCD Teraflops project plans to enhance a commercially available machine with special multiprocessor boards carefully designed to take advantage of the locality features exhibited by QCD calculations (and of many other large scale applications as well)[161]. This supercomputer, with a peak speed of 1.6 Teraflops and an estimated sustained speed in excess of 1 Teraflops, would anticipate the pace of commercial development by a few years and at a fraction of the cost (estimated cost $10M development, $25M construction).

The two projects are quite different and, to a large extent, complementary. The Columbia project is for a rather rigid machine, designed to implement the currently available algorithms in an outstandingly efficient and economical manner. The QCD Teraflops project is for a much more general purpose and easier to program supercomputer, which could be fruitfully used also for a wide range of non QCD applications. The importance that the development and implementation of new algorithms are likely to play for the progress of lattice QCD speaks of course in favor of the flexibility of the QCD Teraflops machine, but the Columbia project has on its side its substantially lower cost.

Since either project would require a substantial allocation of funds, issues of access become important. To formulate these in terms familiar to particle physicists, the question is whether a dedicated machine should be considered more like an accelerator, *i.e.*, a facility to serve several groups of experimenters, or like a detector, where the group who built it is entitled to take and analyze the data in an exclusive manner. Given the expectation that the funds allocated to a QCD machine may, directly or indirectly, reduce the total amount of computer resources otherwise available, many researchers within the lattice community have expressed a strong sentiment that any such machine should be operated as a facility. However, the physicists who design and build a special purpose computer can legitimately expect to see their efforts rewarded by some kind of priority in the use of machine. These are important issues, which will require careful consideration.

6.4.2 Algorithms

Advances in supercomputer technology alone are not sufficient for the progress of lattice QCD. The development of Teraflops supercomputers will bring an increase in computer speed and memory of one to two orders of magnitude with respect to what is available today. The number of operations required by a lattice simulation obviously contains the volume of the lattice as a factor. This implies that a sheer increase of computer power, even into the Teraflop domain, can produce little more than a doubling of the size of the largest lattices that can be studied. As a matter of fact, the situation is worse than that. A major motivation for considering larger lattices is to reduce the lattice spacing, coming closer to the continuum limit. One also wants to be able to consider smaller quark masses. But smaller lattice spacings and smaller quark masses both imply a decrease in computational efficiency, through the phenomenon of critical slowing down. The algorithms for calculating quark propagators (a crucial component of almost all QCD simulations) are based on iterative procedures, whose rate of convergence decreases dramatically as the quark mass (or, better, its value in lattice units $m_q a$) is reduced. Thus, in absence of progress leading to more efficient computational procedures, one cannot expect, from hardware developments alone, even the gains that a naive scaling of the number of degrees of freedom would suggest.

The lattice community has always been aware of the importance of algorithm development and the progress in accuracy of lattice QCD calculations has been accompanied, indeed made possible, by crucial advances in computational techniques. Examples of this progress are all the techniques that have been developed to incorporate fermionic degrees of freedom in the simulations, with the discovery of the "hybrid Monte Carlo" algorithm topping the list of the most important breakthroughs[162]. Another example is given by the refinement in the source and sink operators used for spectroscopy and matrix element calculations. Here, indeed, the line between what should be considered algorithm development and what ought to be considered theoretical progress becomes blurred, but correctly so, because the development of better computational techniques typically finds its roots in a better understanding of the physics of the phenomena under investigation.

Current areas of algorithmic research include the development of better methods for calculating quark propagators, which may overcome, or at least moderate, critical slowing down. Multigrid methods[163] as well as other techniques are being studied. Some progress has been made, but more progress will require a better understanding of the properties of the lattice Dirac operator in presence of fluctuating gauge fields.

Another promising direction of progress consists in the computational use of improved actions[164]. Renormalization group ideas have recently been applied to the definition of a "perfect" action, an action which remains unaltered in the renormalization leading to the continuum limit. Actions approximating the properties of perfect actions may permit to recover the features of the continuum limit working with coarser lattices and therefore with smaller number of dynamical variables. The increased computational power (of the computers of the next generation) could then be applied to an improvement of the accuracy of the simulations and to an expansion of their scope.

6.4.3 Observables

The increase in computer power and the progress in algorithms which are anticipated to occur in a time of three to four years will permit substantial improvements in the accuracy of QCD lattice calculations and a widening of their scope.

One expects that it will be possible to perform quenched calculations of the spectrum for light quark masses close to the experimental value (more properly, for values of m_{ps}/m_{vect} close to m_π/m_ρ). For full QCD, barring unanticipated progress in the algorithms for simulating dynamical fermions, one will probably be able to perform calculations with quark masses half way between m_s and m_u, m_d. This should be sufficient to see the $q-\bar{q}$ vacuum polarization effects go beyond a mere renormalization of the bare coupling constant. One should also be able to see genuine departures from the quenched approximation. Precise determinations of α_S from heavy quark spectroscopy can be expected.

The nature of the transition to a quark-gluon plasma will probably be resolved and progress will be made toward a precise calculation of several thermodynamic observables.

One may expect a rather accurate determination of weak matrix elements (perhaps with errors of $\pm 5\%$) for which one is beginning to get quantitative results, as well as an extension of the calculations to matrix elements which cannot be evaluated today.

More observables will become calculable. These may range from phenomenological parameters, such as the coupling constants in effective chiral Lagrangians, to scattering lengths, to moments of structure functions, to quantities relevant to the interface between perturbative and non-perturbative lattice QCD. While this list of observables is potentially very rich and interesting, it would futile to try to define it too exactly now: its overall span will depend on the detailed progress of the methods of lattice QCD as well as on the ingenuity of the scientists who will apply them.

6.5 Long Range Outlook

Looking farther ahead into the future, given the rapid progress of computer technology and the theoretical and algorithmic developments which are likely to occur, it is to be expected that, five to ten years from now, lattice QCD will be able to produce an accurate determination of a wide range of observables, which will provide stringent tests for the underlying theory of QCD and valuable input for theories describing non-strong interactions. However, the actual rate of progress of lattice QCD will depend on decisions which reflect the policies of the entire particle physics community. This leads us to the following conclusions.

Computer resources - The progress of lattice QCD is heavily dependent on the availability of ever more powerful means of computation. Fortunately the development of supercomputer technology is receiving a lot of support at the policy making level, and thus lattice QCD automatically benefits from the expansion of computer resources that this support generates. Lattice QCD applications, because of the huge volumes of data that they manipulate and the extremely large number crunching capability they require, have been acknowledged as one of the driving forces of supercomputer development. Thus there is the possibility of obtaining funding for QCD applications (either as direct funds for the development of dedicated machines, or in the form of increased allocations of supercomputer time) from non-HEP sources because of the impact that QCD applications may have on supercomputer technology. However, this also requires a strong endorsement from the particle physics community of the value of this mode of research, including the willingness of allocating funds to support the necessary hardware and algorithm developments. While any such investment can be leveraged by appreciable funding from non-HEP sources, it would be difficult to expect the latter to occur if particle physicists, first, do not recognize the value of QCD applications.

Exchange of information - Lattice QCD calculations are not a black box which turns out numbers affected by smaller or larger errors. The details of the calculations are frequently as significant as the final results. On the other hand, lattice QCD investigations are of marginal value if pursued in isolation, without exposure to the whole problematic of strong interactions. Thus, it would be valuable if there were better contacts between scientists working on lattice QCD and other areas.

Experiments - Lattice QCD has the potential of producing one day very accurate results, derived entirely from first principles, on many hadronic observables. It is conceivable, for instance, that it will be possible to predict spectroscopic data with a precision sufficient to put stringent tests to the validity of QCD. However, this would be of little value in absence of experimental data to compare with. As the experimental frontier moves to ever higher energies and smaller distances, it is important not to neglect those energy domains, which do not lie at the boundary of technology, but where a lot of very valuable information can still be collected.

References

[1] B.R. Webber, "QCD and jet physics", in *Proc. of the XXVII International Conference on High Energy Physics*, Glasgow Scotland, July 1994; J. W. Gary, "QCD at high energy colliders", in *Proc. of the Fifth Conference on the Intersections of Particle and Nuclear Physics*, St. Petersburg Florida, Jun 1994.

[2] P.N. Burrows, "QCD at the Z^0", *Nucl. Phys. B* **23** (Proc. Suppl.) 30 (1991); S. Bethke, Aachen preprint PITHA 94/29 (1994) (Talk at the Tennessee International Symposium on Radiative Corrections, Gatlinburg, USA, June 27 - July 1 1994.)

[3] Workshop on physics and experiments with Linear e+e- colliders, Hawaii, 26-30 April 1993, edited F.A. Harris *et al.*, World Scientific, Vol II p. 670.

[4] P.Z. Quintas *et al.*, *Phys. Rev. Lett.* **71** 1307 (1993).

[5] V. Elvira, "Inclusive jet Cross Sections at the DØ Detector", FERMILAB- CONF-94-323C-E, to be published in the proceedings of DPF 1994.

[6] F. Abe *et al.*, *Phys. Rev. Lett.* **69**, 2896 (1992).

[7] F. Nang, "Measurement of the Triple Differential Inclusive DiJet Cross Section, $d^3\sigma/dE_t d\eta_1 d\eta_2$ in $p\bar{p}$ collisions at $\sqrt{s} = 1.8TeV$, FERMILAB-CONF-94-323E-E, to be published in the proceedings of DPF 1994.

[8] G. Wolf, "HERA Physics", DESY 94-022, from the proceedings of the 42nd Scottish Universities Summer School in Physics, 1993; F. Sciulli, "Summary of the Eilat Workshop", DESY 94-147, Eilat, Israel, 1994.

[9] A.P. Bukhvostov, G.V. Frolov, L.N. Lipatov, E.A. Kuraev, *Nucl. Phys. B* **258**, 601 (1985).

[10] V.N. Gribov and L.N. Lipatov, *Sov. J. Nucl. Phys.* **15**, 438 (1972); L. N. Lipatov, *Sov. J. Nucl. Phys.* **20**, 94 (1975); G. Altarelli and G. Parisi, *Nucl. Phys. B* **126**, 298 (1977).

[11] E. Kovacs, "Testing QCD with Jet Physics at CDF", FERMILAB-CONF-94-215-E, to be published in the proceedings of DPF 1994; E. Buckley-Geer, Studies of Prompt Photon Production and Multijet Production at the Tevatron Collider, FERMILAB-CONF-94-336-E to be published in the proceedings of ICHEP, Glasgow, 1994.

[12] "DØ Quantum Chromodynamics: A Compilation of Results Presented at DPF 1994", FERMILAB-Conf-94/323-E DØ; H.Weerts (DØ Collaboration), "Studies of Jet Production with the DØ Detector" in the Proceedings of the 9th Topical Workshop in $p\bar{p}$ Collider Physics, Tsukuba (1993), edited by K.Kondo.

[13] D. Allasia *et al.*, *Phys. Lett. B* **249**, 366 (1990).

[14] "Measurements of Nucleon Structure Functions, F_2 & xF_3, and Precision Tests of PQCD at the FNAL Tevatron", S. R. Mishra *et al.* in *Proceedings of the International Conference on High Energy Physics*, Dallas, TX, August, 1992.

[15] J. Ashman *et al.*, *Nucl. Phys. B* **328**, 1 (1989).

[16] J. Ellis and R. Jaffe, *Phys. Rev. D* **9**, 1444 (1974), erratum-ibid. **10**, 1669 (1974).

[17] P.L. Anthony *et al.*, *Phys. Rev. Lett.* **71**, 959 (1993).

[18] B. Adeva *et al.*, *Phys. Lett. B* **329**, 399 (1994).

[19] B. Adeva *et al.*, *Phys. Lett. B* **320**, 400 (1994).

[20] J. D. Bjorken, *Phys. Rev. D* **1**, 1376 (1970).

[21] K. Abe *et al.*, *Phys. Rev. Lett.* **74**, 346 (1995).

[22] M. Kutschera, *Phys. Lett. B* **325**, 271 (1994).

[23] G.T. Gabadadze, "An Estimate of the Proton Singlet Axial Constant" JINR-E2-94-518, Jan 1995.

[24] "Polarized Protons at RHIC", G. Bunce, J. Collins, S. Heppelmann, R. Jaffe, S.Y. Lee, Y. Makdisi, R.W. Robinett, J. Soffer, M. Tannenbaum, D. Underwood, A. Yokosawa, Particle World Volume 3, No. 1, p. 1-12, 1992.

[25] A. Bhatti, "Inclusive Jet and Two-Jet Differential Cross-Sections at CDF", FERMILAB-CONF-94-159-E, contributed to *27th International Conference on High Energy Physics (ICHEP)*, Glasgow, Scotland, 20-27 Jul 1994.

[26] S. Behrends, "Scaling Behavior of Jet Production in CDF", *Proceedings of Particles & Fields 92: 7th Meeting of the Division of Particles Fields of the APS (DPF 92)*, Batavia, IL, Nov 1992, DPF conf.1992:999-1001 (QCD161:A6:1992).

[27] F. Abe *et al.*, *Phys. Rev. D* **48**, 2998 (1993); *Phys. Rev. Lett.* **73**, 2662 (1994); *Phys. Rev. Lett.* **74**, 1891 (1995).

[28] D. Crane, "*B* Production at CDF", FERMILAB-CONF-93-362-E, Jan 1994, presented at 9th Topical Workshop on Proton - Antiproton Collider Physics, Tsukuba, Japan, 18-22 Oct 1993.

[29] F. Abe *et al.*, *Phys. Rev. Lett.* **71**, 2537 (1993).

[30] S. Abachi *et al.*, "Inclusive μ and B-quark Production Cross-Sections in $\bar{p}p$ Collisions at $\sqrt{s} =$ 1.8 TeV", FERMILAB-PUB-94-409-E, Dec 1994, Submitted to *Phys. Rev. Lett.* .

[31] W. J. Stirling, *Nucl. Phys. B* **423**, 56 (1994).

[32] B. May, "Rapidity Gaps Between Jets at DØ, FERMILAB-CONF-94-323K-E, Sep 1994, presented at *1994 Meeting of the American Physical Society, Division of Particles and Fields (DPF 94)*, Albuquerque, NM, 2-6 Aug 1994.

[33] F. Abe *et al.*, *Phys. Rev. Lett.* **74**, 855 (1995).

[34] S. Catani, L. Trentadue, G. Turnock, B.R. Webber, *Nucl. Phys. B* **407**, 3 (1993).

[35] M. Acciarri *et al.*, *Phys. Lett. B* **345**, 74 (1995); R. Akers *et al.*, *Z. Phys. C* **63**, 197 (1994).

[36] R. Balest *et al.*, "A Study of Jet Production Rates in the Four Flavor Continuum and a Test of QCD", CLEO-CONF-94-28, submitted to Int. Conf . on High Energy Physics, Glasgow, Scotland, Jul 20-27, 1994.

[37] M. R. Adams *et al.*, *Phys. Rev. Lett.* **69**, 1026 (1992).

[38] M. Derrick *et al.*, "Jet Production in high Q^2 Deep-inelastic *ep* Scattering at HERA", DESY-95-016, submitted to *Z. Phys. C* , 1995.

[39] I. Ahmed *et al.*, *Phys. Lett. B* **346**, 415 (1995).

[40] D.J. Miller, "Gamma-gamma Topics and a look at Mesonic Goo", Lepton-Photon Symposium, Cornell, August 1993.

[41] J. Appel, "New Preliminary Results on the Physics of Charm Hadroproduction Subprocesses", FERMILAB-CONF-94-347-E, contrib-

uted to 27th International Conference on High Energy Physics (ICHEP), Glasgow, Scotland, 20-27 Jul 1994.

[42] S. T. Fahey, "Direct Photon Production at DØ", FERMILAB-CONF-94-323A-E, Presented at *1994 Meeting of the American Physical Society, Division of Particles and Fields (DPF 94)*, Albuquerque, NM, Aug 1994.

[43] F. Abe *et al.*, "Direct Photon Results from CDF" FERMILAB-CONF-93-202-E, Submitted to *16th International Symposium on Lepton and Photon Interactions*, Ithaca, NY, Aug 1993.

[44] R. J. Hemingway, "Inclusive particle production in Z0 decays", Proc. of the XXVII International Conference on High Energy Physics, Glasgow Scotland, July 1994

[45] P. N. Burrows, "Measurement of the Charged Multiplicity of $Z^0 \rightarrow B\bar{B}$ Events", SLAC-PUB-6602, Aug 1994. Presented at *1994 Meeting of the American Physical Society, Division of Particles and Fields (DPF 94)*, Albuquerque, NM, Aug 1994.

[46] J. Dominick *et al.*, *Phys. Rev. D* **50**, 4265 (1994).

[47] F. Abe *et al., Phys. Rev. Lett.* **67**, 2937 (1991); *Phys. Rev. Lett.* **66**, 2951 (1991).

[48] J.Zhi-Yu Jiang, "Measurement of the W/Z P_t Distributions at DØ", FERMILAB-CONF-94-323I-E, Sep 1994. 3pp. Presented at *1994 Meeting of the American Physical Society, Division of Particles and Fields (DPF 94)*, Albuquerque, NM, Aug 1994.

[49] M. Derrick *et al., Z. Phys. C* **65**, 379 (1995); I. Abt *et al.*, *Phys. Lett. B* **321**, 161 (1994).

[50] I.M. Dremin, B.B. Levchenko, *Phys. Lett. B* **292**, 155 (1992).

[51] M. Derrick *et al., Phys. Lett. B* **338**, 483 (1994; T. Ahmed *et al., Nucl. Phys. B* **435**, 3 (1995).

[52] G. Ingleman, LHCC Workshop, CERN, Nov., 1994

[53] S.V. Goloskokov, S.P. Kuleshov, O.V. Selyugin, *Mod. Phys. Lett.* A **9**, 1207 (1994).

[54] D. Alde *et al., Phys. Lett. B* **205**, 397 (1988).

[55] S.J. Lindenbaum, "Glueballs in 2++ Final States, Glueballs, Hybrids, and Exotic Hadrons", AIP conf. Proc. no. 185 pp 68-87(1988); S.J. Lindenbaum, "The Status of Glueballs" in *Future Directions in Particle and Nuclear Physics at Multi-Gev Hadron Beam Facilities*, proceedings of the workshop at BNL 4-6 March 1993, BNL-52389, pp. 384-389.

[56] D. Morgan, *Phys. Lett. B* **258**, 444 (1991), erratum-ibid. **269**, 477 (1991).

[57] ATLAS Technical Proposal, CERN/LHCC/94-43, 1994; CMS Technical Proposal, CERN/LHCC/94-38, 1994.

[58] J. C. Collins, D. E. Soper and G. Sterman, "Factorization of Hard Processes in QCD", in *Perturbative Quantum Chromodynamics*, ed. A. H. Mueller, World Scientific (1989).

[59] The CTEQ Collaboration, "Handbook of Perturbative QCD", to be published in Reviews of Modern Physics, 1995.

[60] B. R. Webber, "QCD and Jet Physics" in *Proceedings of the XXVII International Conference on High Energy Physics*, Glasgow, Scotland (1994).

[61] S. Catani, *Proceedings of the International Europhysics Conference on High Energy Physics*, Marseille, France, 22-28 July, 1993.

[62] S. J. Brodsky and G. P. Lepage, "Exclusive Processes in Quantumchromodynamics", in *Perturbative Quantum Chromodynamics*, *op. cit.*

[63] A. S. Carroll *et al., Phys. Rev. Lett.* **61**, 1698 (1988).

[64] A. H. Mueller, "The QCD Perturbation Series" in *QCD 20 Years Later*, eds. P. M. Zerwas and H. A. Kastrup, World Scientific, 1993.

[65] M. A. Shifman, "QCD Sum Rules: The Second Decade" in *QCD 20 Years Later*, *op. cit.*

[66] E. M. Levin "Parton Density at Small x_{bj}" in *QCD 20 Years Later*, *op. cit.*

[67] J. W. Cronin *et al.*, *Phys. Rev. D* **11**, 3105 (1975).

[68] L. Kluberg *et al.*, *Phys. Rev. Lett.* **38**, 670 (1977).

[69] W. Busza and R. Ledoux, *Ann. Rev. Nucl. Part. Sci.* **38**, 119 (1988).

[70] W. Geist, *Nucl. Phys.* A **525**, 149c (1991).

[71] P. M. Fishbane and J. S. Trefil, *Phys. Rev. D* **12**, 2113 (1975).

[72] K. Kastella, *Phys. Rev. D* **36**, 2734 (1987).

[73] K. Kastella, G. Sterman, and J. Milana, *Phys. Rev. D* **39**, 2586 (1989).

[74] D. M. Alde *et al.*, *Phys. Rev. Lett.* **66**, 153 (1991).

[75] P. Amandruz *et al.*, CERN-PPE-91-198 (1991).

[76] R. Vogt, S. J. Brodsky, and P. Hoyer, *Nucl. Phys. B* **360**, 67 (1991).

[77] S. Gavin and J. Milana, *Phys. Rev. Lett.* **68**, 1834 (1992).

[78] C. Benesh, J. Qiu, and J. Vary, preprint ISU-NP-93-15 (1994) ⟨hep-ph/9403265⟩.

[79] S. Gavin, H. Satz, R. L. Thews, and R. Vogt, *Z. Phys. C* **61**, 351 (1994).

[80] J. Qiu and G. Sterman, *Nucl. Phys. B* **353**, 105 and 137 (1991).

[81] M. Luo, J. Qiu, and G. Sterman, *Phys. Rev. D* **49**, 4493 (1994).

[82] M. D. Corcoran *et al.*, *Phys. Lett. B* **259**, 209 (1991).

[83] D. Naples *et al.*, *Phys. Rev. Lett.* **72**, 2341 (1994).

[84] M. Gyulassy, M. Plümer, M. H. Thoma, and X. N. Wang, *Nucl. Phys. A* **538**, 37c (1992).

[85] G. Bertsch, S. J. Brodsky, A. S. Goldhaber, and J. F. Gunion, *Phys. Rev. Lett.* **47**, 297 (1981).

[86] S. J. Brodsky and P. Hoyer, *Phys. Rev. Lett.* **63**, 1566 (1989).

[87] L. L. Frankfurt, G. A. Miller, and M. Strikman, Ann. Rev. Nucl. Part. Sci. **45**, 501 (1994).

[88] M. R. Adams *et al.*, *Phys. Rev. Lett.* **68**, 3266 (1992); *Phys. Lett. B* **287**, 375 (1992).

[89] M. R. Adams *et al.*, *Z. Phys. C* **65**, 225 (1995).

[90] L. McLerran and R. Venugopalan, *Phys. Rev. D* **49**, 2233 and 3352 (1994).

[91] T. Blum, S. Gottlieb, L. Kärkkäinen, and D. Toussaint, preprint AZPH-TH/94-22, ⟨hep-lat/9410014⟩.

[92] R. Pisarski and F. Wilczek, *Phys. Rev. D* **29**, 338 (1984).

[93] F. Wilczek, *Int. J. Mod. Phys. A* **7**, 3911 (1992).

[94] F. R. Brown *et al.*, *Phys. Rev. Lett.* **65**, 2491 (1990).

[95] F. Karsch, preprint BI-TP-95-11 (1995), ⟨hep-lat/9503010⟩.

[96] B. Boyd *et al.*, preprint BI-TP-94-42 (1995), ⟨hep-lat/9501029⟩.

[97] J. Borg, *Nucl. Phys. B* **261**, 455 (1985).

[98] E. Manousakis and J. Polonyi, *Phys. Rev. Lett.* **58**, 847 (1987).

[99] F. Karsch, E. Laermann, and M. Lütgemeier, *Phys. Lett. B* **346**, 94 (1995).

[100] S. Schramm and M. C. Chu, *Phys. Rev. D* **48**, 2279 (1993).

[101] A. D. Linde, Phys. Lett. **96B**, 289 (1980).

[102] A. V. Selikhov and M. Gyulassy, *Phys. Lett. B* . **316**, 373 (1993).

[103] E. Braaten and R. D. Pisarski, *Phys. Rev. D* **42**, 2156 (1990).

[104] C. Gong, *Phys. Lett. B* **298**, 257 (1993); Phys. Rev. D **49**, 2642 (1994).

[105] E. Braaten, *Phys. Rev. Lett.* **74**, 2164 (1995).

[106] J. P. Blaizot and A. H. Mueller, *Nucl. Phys. B* **289**, 847 (1987).

[107] K. J. Eskola, K. Kajantie, and J. Lindfors, Phys. Lett. B **214**, 613 (1988).

[108] K. Geiger and B. Müller, *Nucl. Phys. B* **369**, 600 (1992).

[109] X. N. Wang and M. Gyulassy, *Phys. Rev. D* **44**, 3501 (1991).

[110] T. S. Biró, B. Müller, and X. N. Wang, Phys. Lett. B **283**, 171 (1992).

[111] T. S. Biró *et al.*, Phys. Rev. C **48**, 1275 (1993).

[112] K. Geiger, *QCD based space-time description of heavy ion physics*, Phys. Rept. (in print, 1995).

[113] B. Müller, Rep. Prog. Phys. **28**, 1 (1995).

[114] K. Rajagopal and F. Wilczek, *Nucl. Phys. B* **404**, 577 (1993).

[115] S. Gavin, A. Gocksch, and R. D. Pisarski, *Phys. Rev. Lett.* **72**, 2143 (1994).

[116] M. Asakawa, Z. Huang, and X. N. Wang, *Phys. Rev. Lett.* **74**, 3126 (1995).

[117] M. C. Chu, J. M. Grandy, S. Huang, and J. W. Negele, *Phys. Rev. D* **48**, 3340 (1993); **49**, 6039 (1994).

[118] Experiments 864, 878, 882, 886, and 891 at the AGS at Brookhaven, and NA-52 at the SPS at CERN.

[119] K. P. Pretzl, Europhys. News **24**, 167 (1993).

[120] H. J. Crawford, Sci. Am. **270**, 58 (1994).

[121] J. Gasser and H. Leutwyler, *Nucl. Phys. B* **250**, 465 (1985).

[122] J. Gasser, *Nucl. Phys. B* **279**, 65 (1987).

[123] J. Gasser and H. Leutwyler, Ann. Phys. **158**, 142 (1984).

[124] V. Bernard *et al.*, Phys. Rept. **246**, 315 (1994).

[125] S. Weinberg, *Nucl. Phys. B* **363**, 3 (1991); *Phys. Lett. B* **295**, 114 (1992).

[126] C. Ordonez and U. van Kolck, *Phys. Lett. B* **291**, 459 (1991).

[127] C. Ordonez, L. Ray, and U. van Kolck, *Phys. Rev. Lett.* **72**, 1982 (1994).

[128] M. Knecht, B. Moussallam, and J. Stern, *Nucl. Phys. B* **429**, 125 (1994).

[129] E. Jenkins and A. V. Manohar, Phys. Lett B **255**, 558 (1991); **259**, 353 (1991).

[130] G. 't Hooft, *Nucl. Phys. B* **72**, 461 (1974); **75**, 461 (1974).

[131] E. Witten, *Nucl. Phys. B* **160**, 57 (1979).

[132] M. P. Mattis and M. E. Peskin, *Phys. Rev. D* **32**, 58 (1985).

[133] R. Dashen and A. V. Manohar, *Phys. Lett. B* **315**, 425 and 438 (1993).

[134] *Proceedings of Lattice 90-94*, *Nucl. Phys. B* (Proc. Suppl.) 20 (1991); 26 (1992); 30 (1993); 34 (1994); 42 (1995).

[135] K. Wilson, *Phys. Rev. D* **10**, 2445 (1974).

[136] M. Creutz, L. Jacobs and C. Rebbi, Phys. Rep. **95**, 201 (1983).

[137] H. B. Nielsen and M. Ninomiya, *Nucl. Phys. B* **185**, 20 (1981); *Nucl. Phys. B* **195**, 541 (1982).

[138] J. Kogut and L. Susskind, *Phys. Rev. D* **11**, 395 (1975).

[139] L. Susskind, *Phys. Rev. D* **16**, 3031 (1977).

[140] A. Hasenfratz and P. Hasenfratz, Phys. Lett. **93B**, 165 (1980).

[141] R. Dashen and G. Gross, *Phys. Rev. D* **23**, 2340 (1981).

[142] H. Hamber and G. Parisi, *Phys. Rev. Lett.* **47**, 1792 (1981).

[143] D. Weingarten, *Phys. Lett. B* **109**, 57 (1982).

[144] C. Michael, *Proceedings of Lattice 94 Nucl. Phys. B* **42**, (Proc. Suppl.): 147 (1995).

[145] F. Butler, H. Chen, J. Sexton, A. Vaccarino and D. Weingarten, *Nucl. Phys. B* **430**, 179 (1994).

[146] G. Bali *et al.*, *Phys. Lett. B* **309**, 378 (1993).

[147] J. Sexton, A. Vaccarino and D. Weingarten, *Proceedings of Lattice 94*, *Nucl. Phys. B* **42** (Proc. Suppl.): 279 (1995).

[148] P. MacKenzie, *Proceedings of Lattice 92*, *Nucl. Phys. B* **30** (Proc. Suppl.): 35 (1993).

[149] A. El-Khadra, *Proceedings of Lattice 93*, *Nucl. Phys. B* **34** (Proc. Suppl.): 141 (1994).

[150] A. Ukawa, *Proceedings of Lattice 89*, *Nucl. Phys. B* **17** (Proc. Suppl.): 118 (1990).

[151] B. Peterson, *Proceedings of Lattice 92*, *Nucl. Phys. B* **30** (Proc. Suppl.): 66 (1993).

[152] F. Karsch, *Proceedings of Lattice 93*, *Nucl. Phys. B* **34** (Proc. Suppl.): 63 (1994).

[153] C. De Tar, *Proceedings of Lattice 94*, *Nucl. Phys. B* **42** (Proc. Suppl.): 73 (1995).

[154] C. Sachrajda, *Proceedings of Lattice 92*, *Nucl. Phys. B* **30** (Proc. Suppl.): 20 (1993).

[155] C. Bernard, *Proceedings of Lattice 93*, *Nucl. Phys. B* **34** (Proc. Suppl.): 47 (1994).

[156] G. Martinelli, *Proceedings of Lattice 94*, *Nucl. Phys. B* **42** (Proc. Suppl.): 127 (1995).

[157] S. Sharpe, *Proceedings of Lattice 93*, *Nucl. Phys. B* **34** (Proc. Suppl.): 403 (1994).

[158] K. Wilson, T. Walhout, A. Harindranath, W-M. Zhang, R. Perry and S. Glazek, *Phys. Rev. D* **49**, 6720 (1994).

[159] Y. Iwasaki, *Proceedings of Lattice 93*, *Nucl. Phys. B* **34** (Proc. Suppl.): 78 (1994).

[160] R. Mawhinney, *Proceedings of Lattice 94*, *Nucl. Phys. B* **42** (Proc. Suppl.): 140 (1995).

[161] J. Negele, *Proceedings of Lattice 92*, *Nucl. Phys. B* **30** (Proc. Suppl.): 295 (1993).

[162] S. Duane, A. Kennedy, B. Pendleton, D. Roweth, *Phys. Lett. B* **195**, 216 (1987).

[163] R. Brower, R. Edwards, C. Rebbi and E. Vicari, *Nucl. Phys. B* **366**, 689 (1991).

[164] T. DeGrand, A. Hasenfratz, P. Hasenfratz, F. Niedermayer and U. Wiese, *Proceedings of Lattice 94*, *Nucl. Phys. B* **42** (Proc. Suppl.): 67 (1995).

Appendix: DPF QCD Workshop Agenda

Saturday, April 9, 1994 University of Wisconsin, Madison, WI

QCD Experimental Session - Organizer: Wesley Smith, University of Wisconsin

8:30 - 8:40	Wesley Smith	U of Wisconsin	Introduction
8:40 - 9:00	Bill Gary	UC Riverside	LEP
9:00 - 9:20	Phil Burrows	MIT	SLD
9:20 - 9:40	Sukhpal Sanghera	Cornell	CLEO
9:40 - 10:00	Steve Geer	FNAL	CDF
10:00 - 10:20	Harry Weerts	Michigan State	DØ
10:20 - 10:40	Allen Caldwell	Columbia U.	HERA
11:00 - 11:20	Harry Melanson	FNAL	FNAL-E665
11:20 - 11:40	Janet Conrad	Columbia U.	FNAL-E815
11:40 - 12:00	Emlyn Hughes	SLAC	SLAC-E142
12:00 - 12:20	Richard Milner	MIT	HERA-HERMES
12:20 - 12:40	Alex Dzierba	Indiana U.	Light Quark Spectroscopy
12:40 - 13:00	Wu-Ki Tung	Michigan State	CTEQ
14:00 - 14:20	Jim Carroll	LBL	RHIC-STAR
14:20 - 14:40	Joel Moss	Los Alamos	RHIC-PHENIX
14:40 - 14:50	Gerry Bunce	BNL	RHIC-SPIN
14:50 - 15:00	Wlodek Guryn	BNL	RHIC-pp elastic
15:00 - 15:10	Bolek Wyslouch	MIT	RHIC-PHOBOS

Lattice Gauge Session - Organizer: Claudio Rebbi, Boston University

15:30 - 16:00	Norman Christ	Columbia U.	Solving QCD: Why, How, When?
16:00 - 16:30	Greg Kilcup	Ohio State	Weak Matrix Elements
16:30 - 17:00	Andreas Kronfeld	FNAL	SM Phenomenology & Lattice QCD
17:00 - 17:30	Jeff Mandula	D.O.E.	Resources & Impact of L.G.T.
17:30 - 18:00	John Negele	MIT	Teraflops Project
18:00 - 18:30	Doug Toussaint	U. of Arizona	Numerical Calculations in QCD

Sunday, April 10, 1994

QCD Theory Session - Organizer: Berndt Muller, Duke University

8:00 - 8:30	Registration/Coffee & Pastries		
8:30 - 9:00	Joe Kapusta	U. of Minnesota	Finite T. QCD
9:00 - 9:30	Berndt Muller	Duke	RHIC - QCD Theory
9:30 - 10:00	K. Rajagopal	Harvard	Chiral Phase Transition
10:00 - 10:30	J. Qiu	Iowa State	QCD & A-Dep in Had-Nucleus
10:30 - 10:35	N. Chang	CCNY	Chiral Restoration at High-T

QCD Theory Session - Organizer: Al Mueller, Columbia University

11:00 - 11:30	George Sterman	Stony Brook	In face of Pert. & Non-Pert. QCD
11:30 - 12:00	John Collins	Penn State	Polarization & QCD
12:00 - 12:30	Steve Ellis	U. Washington	JETS: Past, Present, Future
13:30 - 14:00	Genya Levin	FNAL	small-x and Diffractive Phys.
14:00 - 14:30	Lance Dixon	SLAC	H0 Multi-parton Calculations
14:30 - 14:45	Paul Stevenson	Rice University	Scheme dep., opt. & Freezing
14:45 - 15:00	Sam Lindenbaum	BNL	Glueball Investigations